Mon. Not. R. astr. Soc. (1989) **240**, 881–915

The high-overtone *p*-mode spectrum of the rapidly oscillating Ap star HR 1217 (HD 24712) – results of a frequency analysis of 324 hr of multi-site photometric observations obtained during a 46-d time-span in 1986★

D. W. Kurtz *Department of Astronomy, University of Cape Town, Rondebosch 7700, South Africa*

J. M. Matthews† *Department of Astronomy, University of Western Ontario, London, Ontario N6A 3K7, Canada*

P. Martinez and J. Seeman *Department of Astronomy, University of Cape Town, Rondebosch 7700, South Africa*

Mark Cropper‡ *Anglo-Australian Observatory, PO Box 296, Epping, NSW 2121, Australia*

J. Christopher Clemens *Department of Astronomy, University of Texas, Austin, TX 78712, USA*

T. J. Kreidl *Lowell Observatory, 1400 W. Mars Hill Rd, Flagstaff, AZ 86001, USA*

C. Sterken§ *Astrophysical Institute, Vrije Universiteit Brussel, Pleinlaan 2, B-1050 Brussel, Belgium*

H. Schneider *Universitats-Sternwarte Geismarlandstrasse 11 D-3400 Göttingen, FRG*

W. W. Weiss *Institut für Astronomie, Türkenschanzstrasse 17, A-1180 Wien, Austria*

Steven D. Kawaler¶ *Yale University, Center for Solar and Space Research, PO Box 6666, New Haven, CT 06511, USA*

S. O. Kepler¶ *Instituto de Fisica, Universidade Federal do Rio Grande do Sul, 90049 Porto Alegre RS, Brazil*

★Based on observations obtained at Cerro Tololo Inter-American Observatory, European Southern Observatory, Lowell Observatory, McDonald Observatory, Mauna Kea Observatory, Mount John Observatory, Mount Stromlo and Siding Spring Observatory, and South African Astronomical Observatory. Observations at ESO were obtained in part within the framework of the European Ap star working group.

†Current address: Department of Geophysics and Astronomy, University of British Columbia, Vancouver, British Columbia, V6T 2A5, Canada.

‡Current address: Mullard Space Science Laboratory, Holmbury St Mary, Dorking, Surrey RH5 6NT.

§Senior Research Associate NFWO-Belgium.

¶Visiting astronomer, Cerro Tololo Inter-American Observatory, operated by the Associated Universities for Research in Astronomy, Inc., under contract with the National Science Foundation.

A. van der Peet and D. J. Sullivan *Physics Department, Victoria University of Wellington, New Zealand*

H. J. Wood‖ *Cerro Tololo Inter-American Observatory, Casilla 603, La Serena 1353, Chile*

Accepted 1989 April 5. Received 1989 March 20

Summary. We present new high-speed photometric observations of the rapidly oscillating Ap star HR 1217 obtained during 365 hr of observation at eight observations in 1986 October, November and December. We show that the 6-min light variations are amplitude modulated in phase with the magnetic variations, with amplitude maximum and magnetic maximum coinciding; mean light minimum occurs at a slightly, but probably significantly, different time. A frequency analysis of 324 hr of those observations over a 46-d time-span yields six principal frequencies, all of which are amplitude modulated with the rotation of the star. The duty cycle for this dataset is 29 per cent; the 3 d^{-1} (34 μHz) aliases, which have previously caused the failure of frequency analyses of data obtained at a single site, are only 12 per cent in amplitude of the central peak of the spectral window and cause little problem. We find:

(i) HR 1217 is an oblique rotator with a centred dipole magnetic field.

(ii) HR 1217 is an oblique pulsator with the pulsation axis and the magnetic axis aligned.

(iii) There are six principal frequencies of pulsation in HR 1217. We find that ν_2 and ν_4 are dipole modes ($l=1$, $m=0$); ν_3 and ν_5 cannot be described by single spherical harmonics – they look similar to dipole modes, but they have amplitude minima which are lower than expected.

(iv) It is not possible to discriminate between the hypothesis that ν_1, ν_2, ν_3, ν_4 and ν_5 are basically due to alternating even and odd l-modes with $\nu_0=68$ μHz, and the hypothesis that they are basically due to dipole modes with $\nu_0=34$ μHz.

(v) The secondary frequencies indicate that the principal frequencies are amplitude modulated on a time-scale of months. This is not likely to be due to pulsation in higher degree modes, and hence indicates that the amplitudes of the principal frequencies are not completely stable. The frequency spectrum of HR 1217 is qualitatively similar to that of the sun and presents a wealth of intriguing problems.

1 Introduction

HR 1217 is one of the coolest of the SrCrEu Ap stars, with an effective temperature equivalent to a normal spectral type of about F0. Its magnetic field was studied by Preston (1972), who found that it varies with a period of 12.448 d, with no polarity reversal. More recent magnetic observations using Hβ polarimetry in 1983 (Landstreet, private communication) combined

‖Current address: NASA Goddard Space Flight Center, Optical Test Section, Code 717.3, Greenbelt, MD, 20771, USA.

with those of Preston indicate that the range of the variation is from $+413 \pm 53$ G to $+1317 \pm 53$ G; the shape of the variation is sinusoidal to within the observational errors (see Section 5.1). Preston also found that HR 1217 has significant spectrum variations with maximum Eu line strength coinciding with magnetic maximum, and maximum Mg, Ti, Cr and Fe line strengths coinciding with magnetic minimum.

Wolff & Morrison (1973) studied the mean* light variations of HR 1217 in the Strömgren system. They found that mean light minimum coincides with Eu line strength maximum for all four Strömgren filters. Bonsack (1979) measured line-blocking coefficients across the visible part of the spectrum over the rotation period. He found that the surface distribution of the elements does not appear to be concentric about the visible magnetic pole, but rather seems to be spread along a ridge which stretches behind the pole by about 50° in longitude.

Kurtz (1982) obtained mean light observations in Johnson *B* and Kurtz & Marang (1987) obtained mean light observations in *UBVRI*. By combining the Eu line-strength observations and the photometric observations, Kurtz & Marang determined the rotation period of HR 1217 to be 12.4572 ± 0.0003 d. They also suggested that the time of mean light minimum may not coincide with the time of magnetic maximum; they found a difference between the two of 1.00 ± 0.34 d.

HR 1217 was discovered to be a rapidly oscillating Ap star by Kurtz (1982). He found that it oscillates in more than one mode simultaneously with periods near 6 min and with a maximum peak-to-peak light variation of about 10 mmag through a Johnson *B* filter. He also found that the pulsation amplitude is modulated with the rotation of the star so that maximum pulsation amplitude coincides with maximum magnetic field strength. His frequency analysis of 63 hr of high-speed photometric observations of HR 1217 obtained in 1980/1981 was severely affected by the alias pattern of the spectral window resulting from observations obtained from only a single observing site, and he was unable to determine the pulsation frequencies with certainty. Nevertheless, the frequencies which he found appeared to be amplitude modulated with the rotation period of the star, giving rise to rotational sidelobes to those frequencies.

That amplitude modulation was interpreted by Kurtz (1982) in terms of the oblique pulsator model, in which he assumed that the axis of oscillation is coincident with the magnetic axis, which is itself oblique to the rotation axis. (Throughout this paper we will refer to the frequencies which we assume are due to independent pulsation modes as the principal frequencies; in the oblique pulsator model the rotational sidelobes are descriptive of the amplitude modulation of the principal frequencies and are not due to independent pulsation modes.) The oblique pulsator model has since been refined by Dziembowki & Goode (1985, 1986), Shibahashi (1986) and Kurtz & Shibahashi (1986) to take into account the effects of both the Coriolis force and magnetic field.

Mathys (1985) suggested an alternative model, the spotted pulsator model, which has additional free parameters. Since HR 1217 does have mean light variations of a few per cent, there is at least that small effect which can be interpreted within the spotted pulsator model. Matthews *et al.* (1988) detected radial velocity variations of $400\,\mathrm{m\,s^{-1}}$ peak-to-peak in HR 1217 during two nights in 1986 December simultaneous with high-speed photometric observations presented in this paper. Those radial velocity variations prove conclusively that HR 1217 is pulsating. They are also amplitude modulated in a manner consistent with the oblique pulsator model.

*Throughout this paper we will refer to the light variations which occur on the rotation time-scale of 12.4572 d as mean light variations. This is in order to distinguish them from the rapid light variations which occur on a time-scale of 6 min.

In principle, within the oblique pulsator model, the relative ratios of the amplitudes of the principal frequencies and their rotational sidelobes allow identification of the degree, l, of the modes; provide information on the rotational inclination of the star, i; the magnetic obliquity, β; the rotational frequency, $\nu_{\rm rot}$; and an integrated measure of the internal magnetic field strength. In addition, the frequency spacing between the principal frequencies provides information about the internal structure of the star. To extract all of the possible information from the oscillations, a complete frequency analysis is necessary.

Kurtz & Seeman (1983) obtained high-speed photometric observations of HR 1217 contemporaneously from the South African Astronomical Observatory (SAAO) and the Cerro Tololo Inter-American Observatory (CTIO). To reduce the complication of the frequency analysis induced by the rotational amplitude modulation, they concentrated their analysis on four nights which were centred on the time of amplitude maximum. They found at least five, and possibly six, frequencies which were roughly equally spaced; they suggested that these frequencies were due to eigenmodes of consecutive overtone, n, with n in the range 76–81.

The asymptotic relationship for the frequency spacing of high-overtone ($n \gg 1$) p-modes (Tassoul 1980) can be written as

$$\nu_{n,l} \approx \nu_0\{(n+l/2+\varepsilon)-[l(l+1)+\delta]A/(n+l/2+\varepsilon)\}, \quad (1)$$

where $1/\nu_0$ is the sound travel-time from the surface to the centre and back and ε, δ and A are constants which depend on stellar structure. The sound travel-time increases as a star evolves off the main sequence both because of increasing radius and because of decreasing density which decreases sound speed and hence decreases ν_0.

Shibahashi (1984) pointed out that the frequency spacing found by Kurtz & Seeman, $\approx 34\ \mu$Hz, indicates that HR 1217 has evolved out of the main-sequence band. He suggested that the observed frequency spacing is half the value for consecutive overtones, $\nu_0/2$, and that the observed frequencies are due to alternating even and odd l-modes with $\nu_0 = 68\ \mu$Hz. Model calculations of ν_0 (Shibahashi & Saio 1985; Gabriel *et al.* 1985; Heller & Kawaler 1988) place HR 1217 1.5 mag above the main sequence if $\nu_0 = 34\ \mu$Hz, and 0.3 mag above it if $\nu_0 = 68\ \mu$Hz. If we assume that an F0 zero-age main-sequence star has a radius of 1.4 $R_\odot$, then the former implies a radius of $R = 3.2\ R_\odot$ and the latter implies $R = 2.3\ R_\odot$. Is there a way to discriminate between these two possibilities?

The radius of HR 1217 is not known independently of the above arguments and the radii of Ap stars, in general, are only known statistically, except for a few cases. Preston (1970) calculates that, on average, $R = 3.2\ R_\odot$ for the Ap stars he studied, but $R = 2.3\ R_\odot$ certainly seems to obtain for some stars. We cannot, therefore, distinguish between $\nu_0 = 34\ \mu$Hz and $\nu_0 = 68\ \mu$Hz on the basis of any knowledge or expectation of the radius, and hence luminosity, of HR 1217. Heller & Kawaler (1988) point out that if HR 1217 is a luminosity class III star, the principal frequencies should be changing at a rate which is measurable with only about 5 yr of observations. In principle, then, there is an observational test to distinguish whether ν_0 is 34 or 68 μHz and hence determine the luminosity and age of HR 1217. In practice, as we will show in Section 4.5, we cannot yet do that because of resolution problems in the frequency analysis.

The separations of the principal frequencies found by Kurtz & Seeman (1983) are not exactly equal. If we assume that the alternating even and odd l-mode interpretation of the principal frequencies suggested by Shibahashi is correct (i.e. $\nu_0 = 68\ \mu$Hz), then this inequality in the frequency spacing is due to the effect of the second term in equation (1). In particular, $(\nu_{n,1} - \nu_{n,0}) < (\nu_{n+1,0} - \nu_{n,1})$ and $(\nu_{n,1} - \nu_{n-1,2}) > (\nu_{n,2} - \nu_{n,1})$. This was pointed out by Shibahashi & Saio (1985) who suggested that the modes with even l were likely to be $l = 0$ rather than $l = 2$.

In order to test this suggestion, Kurtz, Schneider & Weiss (1985) obtained contemporaneous high-speed photometric observations of HR 1217 from SAAO and the European Southern Observatory (ESO) on four nights centred on the time of amplitude (magnetic) minimum. They were able to show that all of the frequencies found by Kurtz & Seeman are amplitude modulated and hence none can be due to radial ($l=0$) modes.

All of the above suggests a clear need for a definitive frequency analysis of HR 1217. Such an analysis can, in principle, provide information on the luminosity, mass, age, evolutionary time-scale, interior structure, internal magnetic field strength, rotational period, rotational inclination and magnetic obliquity of the star. The apparent pattern of frequencies seen in the analysis of Kurtz & Seeman (1983) bears a close resemblance to the solar high-overtone p-mode frequency pattern, hence HR 1217 is a logical candidate for an intensive observational study in order to apply the techniques of asteroseismology (starting with equation 1).

Gathering sufficient observations of HR 1217 to obtain a definitive frequency analysis is not easy, however. The principal frequencies are separated by about $34\,\mu\text{Hz} = 2.94\,\text{d}^{-1} \approx 3\,\text{d}^{-1}$. For observations taken from a single observing site the window pattern has $3\,\text{d}^{-1}$ aliases of such large amplitude that the frequency pattern is hopelessly confused. Kurtz's (1982) initial analysis suffered from this problem and both principal frequencies he selected are incorrect by $1\,\text{d}^{-1}$. In addition, we know that the amplitudes of the principal frequencies in HR 1217 are modulated with the rotation period (or something very near to the rotation period) of $P_{\text{rot}} = 12.4572$ d. We expect that if HR 1217 is an oblique pulsator, as other rapidly oscillating Ap stars appear to be (Kurtz 1986), and if each of the principal frequencies is due to pulsation in a normal mode,* then each will be split into $(2l+1)$ observable frequencies separated by ν_{rot} (see Shibahashi 1986; Kurtz & Shibahashi 1986). Good phase coverage is therefore necessary over the entire rotation cycle of 12.4572 d. Given the vagaries of weather and the realities of telescope scheduling, observations spanning several rotation cycles are necessary in order to assure good rotational phase coverage.

To overcome these problems we organized a multi-site observational campaign on HR 1217 for three months in 1986: October, November and December. We obtained 365 hr of high-speed photometric observations under good photometric conditions from eight observatories on 55 nights during those 3 months. During a time-span of 46 d (3.7 rotation cycles) we obtained 324 hr of observations through Johnson *B* filters for a duty cycle of 29 per cent. In this paper we present those new observations in addition to all previous high-speed photometric observations of HR 1217 which are in our possession, both published and unpublished, and we present the results of a frequency analysis of those data.

2 Observations

Table 1 gives a journal of all of the high-speed photometric observations of HR 1217 which are in our possession. These data have been deposited in machine readable form in the *IAU archives of unpublished photoelectric observations of variable stars* at the Centre de Données Stellaires, Observatoire de Strasbourg, as file number C2 (see Breger 1988). The data from JD2444540–2444643 are from Kurtz (1982); from JD2444849–2444953 are from Kurtz & Seeman (1983); from JD2445661–2445664 are from H. J. Wood (unpublished); from JD2445690–2445693 are from Kurtz, Schneider & Weiss (1985). The rest of the observations from JD2446712–2446784 were obtained in the multi-site campaign for this paper.

Most of the observations have been obtained through a Johnson *B* filter. Studies of the relative amplitude of the light variations as a function of filter for several rapidly oscillating Ap

*Throughout this paper we will use the term 'normal mode' to refer to a mode which can be described by a single spherical harmonic.

Table 1. Journal of observations of HR 1217.

Date		JD	N 40-s	t hr	σ mmag	Obs	Fil	Tel	Obsr
1980									
October	27/28	2444540	214	2.48	2.43	WO	*b*	1.0-m	DWK
November	0/1	2444544	236	2.72	2.10	WO	*b*	1.0-m	DWK
December	2/3	2444576	336	4.24	3.10	SAAO	B	0.5-m	DWK
December	3/4	2444577	442	5.51	2.71	SAAO	B	0.5-m	DWK
December	4/5	2444578	406	5.12	2.42	SAAO	B	0.5-m	DWK
December	5/6	2444579	360	4.55	2.23	SAAO	B	0.5-m	DWK
December	7/8	2444581	183	2.32	1.79	SAAO	B	0.5-m	DWK
December	8/9	2444582	357	4.52	1.19	SAAO	B	0.5-m	DWK
December	9/10	2444583	372	4.75	1.94	SAAO	B	0.5-m	DWK
December	10/11	2444584	324	4.10	1.81	SAAO	B	0.5-m	DWK
December	11/12	2444585	320	4.06	2.00	SAAO	B	0.5-m	DWK
Σ			3550	44.37					
1981									
January	12/13	2444617	162	2.07	2.25	SAAO	B	0.5-m	DWK
January	14/15	2444619	132	1.68	1.36	SAAO	B	0.5-m	DWK
January	15/16	2444620	134	1.67	1.96	SAAO	B	0.5-m	DWK
January	16/17	2444621	173	2.18	2.01	SAAO	B	0.5-m	DWK
January	17/18	2444622	163	2.03	1.28	SAAO	B	0.5-m	DWK
January	18/19	2444623	71	0.88	1.66	SAAO	B	0.5-m	DWK
January	19/20	2444624	150	1.88	2.21	SAAO	B	0.5-m	DWK
February	3/4	2444639	85	1.33	2.82	SAAO	B	0.5-m	DWK
February	4/5	2444640	96	1.20	2.41	SAAO	B	0.5-m	DWK
February	5/6	2444641	100	1.24	1.86	SAAO	B	0.5-m	DWK
February	6/7	2444642	91	1.12	1.85	SAAO	B	0.5-m	DWK
February	7/8	2444643	70	0.86	2.35	SAAO	B	0.5-m	DWK
September	1/2	2444849	87	1.09	2.93	SAAO	B	0.5-m	DWK
September	2/3	2444850	300	3.72	2.57	SAAO	B	0.5-m	DWK
September	3/4	2444851	349	4.32	3.21	SAAO	B	0.5-m	DWK
September	4/5	2444852	351	4.35	2.82	SAAO	B	0.5-m	DWK
September	15/16	2444863	40	0.49	3.32	SAAO	B	0.5-m	DWK
September	18/19	2444866	319	4.05	2.36	SAAO	B	0.5-m	DWK
September	19/20	2444867	349	4.40	1.75	SAAO	B	0.5-m	DWK
September	20/21	2444868	253	3.17	1.44	SAAO	B	0.5-m	DWK
September	21/22	2444869	365	4.65	1.86	SAAO	B	0.5-m	DWK
October	27/28	2444905	462	5.46	1.58	SAAO	B	0.5-m	DWK
October	29/30	2444907	410	4.82	1.55	SAAO	B	0.5-m	DWK
November	2/3	2444911	484	5.86	2.76	SAAO	B	0.5-m	DWK
November	18/19	2444927	351	4.62	2.73	SAAO	B	0.5-m	DWK
November	19/20	2444928	474	6.34	2.21	SAAO	B	0.5-m	DWK
November	20/21	2444929	190	2.35	1.97	SAAO	B	0.5-m	DWK
November	23/24	2444932	497	6.28	1.63	SAAO	B	0.5-m	DWK
December	8/9	2444947	169	2.15	2.15	SAAO	B	0.5-m	DWK
December	9/10	2444948	345	4.57	3.05	SAAO	B	0.5-m	DWK
December	10/11	2444949				CTIO	B	0.4-m	DWK
December	10/11	2444949	913	11.59	3.38	SAAO	B	0.5-m	JS
December	11/12	2444950				CTIO	B	0.4-m	DWK
December	11/12	2444950	637	8.12	3.21	SAAO	B	0.5-m	JS
December	12/13	2444951				CTIO	B	0.4-m	DWK
December	12/13	2444951	656	8.14	3.03	SAAO	B	0.5-m	JS
December	13/14	2444952				CTIO	B	0.4-m	DWK
December	13/14	2444952	625	7.91	2.56	SAAO	B	0.5-m	JS
December	14/15	2444953				CTIO	B	0.4-m	DWK
December	14/15	2444953	838	10.61	2.82	SAAO	B	0.5-m	JS
Σ			10891	137.20					
1983									
November	22/23	2445661	377	4.72	2.85	CTIO	B	0.9-m	HJW
November	23/24	2445662	397	4.70	2.56	CTIO	B	0.9-m	HJW
November	25/26	2445664	324	3.81	2.06	CTIO	B	0.9-m	HJW
December	21/22	2445690	287	3.96	1.64	ESO	B	0.9-m	HS/WWW
December	22/23	2445691	354	4.78	1.94	SAAO	B	0.75-m	DWK
December	23/24	2445692				SAAO	B	0.75-m	DWK
December	23/24	2445692	492	6.83	1.98	ESO	B	0.9-m	HS/WWW
December	24/25	2445693				SAAO	B	0.75-m	DWK
December	24/25	2445693	316	84.27	2.12	ESO	B	0.9-m	HS/WWW
Σ			2547	33.07					

Table 1 — *continued*

Date		JD	N 40-s	t hr	σ mmag	Obs	Fil	Tel	Obsr
1986									
October	8/9	2446712	56	0.62	1.45	SAAO	B	1.0-m	DWK
October	9/10	2446713	137	1.56	1.89	SAAO	B	1.0-m	DWK
October	10/11	2446714	118	1.33	1.78	SAAO	B	1.0-m	DWK
October	11/12	2446715	145	2.14	1.95	ESO	B	0.9-m	HS/WWW
October	12/13	2446716	221	2.94	2.31	ESO	B	0.9-m	HS/WWW
October	14/15	2446718	194	3.04	2.45	ESO	B	0.9-m	HS/WWW
October	19/20	2446723	261	3.63	1.54	ESO	B	0.6-m	HS/WWW
October	20/21	2446724	270	3.63	1.52	ESO	B	0.6-m	HS/WWW
October	21/22	2446725	44	0.53	1.30	ESO	B	0.6-m	HS/WWW
October	22/23	2446726	204	3.28	1.46	ESO	B	0.6-m	HS/WWW
October	23/24	2446727	206	2.68	1.52	ESO	B	0.6-m	HS/WWW
October	24/25	2446728	86	1.04	2.06	ESO	B	0.6-m	HS/WWW
November	3/4	2446738	447	6.20	2.03	MSSSO	B	0.6-m	MSC
November	4/5	2446739	157	2.83	3.41	MSSSO	B	0.6-m	MSC
November	4/5	2446739	476	5.39	2.20	SAAO	B	1.0-m	DWK
November	5/6	2446740	650	7.33	2.01	SAAO	B	1.0-m	DWK
November	6/7	2446741	427	4.80	2.73	SAAO	B	1.0-m	DWK
November	8/9	2446743	206	2.45	3.54	MSSSO	B	0.6-m	MSC
November	8/9	2446743	354	4.24	2.88	LO	BV	1.1-m	TJK
November	9/10	2446744	588	6.81	4.21	MSSSO	B	0.6-m	MSC
November	9/10	2446744	649	7.31	2.87	SAAO	B	1.0-m	DWK
November	9/10	2446744	179	2.10	2.68	LO	BV	1.1-m	TJK
November	10/11	2446745	666	7.49	2.66	SAAO	B	1.0-m	DWK
November	10/11	2446745	324	3.88	2.38	LO	BV	1.1-m	TJK
November	11/12	2446746	633	7.13	2.47	SAAO	B	1.0-m	DWK
November	12/13	2446747	612	7.31	1.83	SAAO	B	1.0-m	DWK
November	12/13	2446747	526	7.07	2.73	CTIO	B	1.0-m	SDK/SOK
November	12/13	2446747	360	4.26	2.16	LO	BV	1.1-m	TJK
November	13/14	2446748	693	7.83	1.64	SAAO	B	1.0-m	DWK
November	13/14	2446748	584	6.84	2.14	CTIO	B	1.0-m	SDK/SOK
November	14/15	2446749	551	6.22	1.48	SAAO	B	1.0-m	DWK
November	15/16	2446750	693	7.84	1.65	SAAO	B	1.0-m	DWK
November	15/16	2446750	508	6.28	1.75	CTIO	B	0.6-m	SDK/SOK
November	16/17	2446751	685	7.70	1.63	SAAO	B	1.0-m	DWK
November	17/18	2446752	392	4.67	1.80	SAAO	B	1.0-m	DWK
November	18/19	2446753	544	6.25	4.91	SAAO	B	1.0-m	DWK
November	19/20	2446754	205	2.32	1.99	SAAO	B	1.0-m	PM
November	21/22	2446756	468	5.53	3.47	SAAO	B	1.0-m	PM
November	21/22	2446756	232	2.73	2.28	ESO	uvby	0.5-m	CS
November	21/22	2446756	555	6.17	3.12	MDO	B	0.75-m	JCC
November	22/23	2446757	533	5.93	2.70	ESO	uvby	0.5-m	CS
November	23/24	2446758	458	5.18	2.65	SAAO	B	1.0-m	PM
November	24/25	2446759	377	4.20	2.29	ESO	uvby	0.5-m	CS
November	24/25	2446759	572	6.38	2.71	MDO	B	0.75-m	JCC
November	25/26	2446760	116	1.38	1.98	ESO	uvby	0.5-m	CS
November	25/26	2446760	343	3.81	2.29	MDO	B	0.75-m	JCC
November	26/27	2446761	197	2.90	1.93	SAAO	B	0.75-m	JS
November	27/28	2446762	118	2.02	1.73	SAAO	B	0.75-m	JS
November	28/29	2446763	150	1.75	1.44	SAAO	B	0.75-m	JS
November	28/29	2446763	321	3.70	2.36	MJO	B	0.6-m	AvdP/DJS
November	29/30	2446764	596	6.85	2.29	SAAO	B	0.75-m	JS
December	0/1	2446765	411	5.27	2.45	SAAO	B	0.75-m	JS
December	1/2	2446766	552	6.58	2.38	SAAO	B	0.75-m	JS
December	2/3	2446767	541	6.50	2.61	SAAO	B	0.75-m	PM
December	2/3	2446767	172	2.30	2.58	MJO	B	0.6-m	AvdP/DJS
December	3/4	2446768	589	6.87	2.51	SAAO	B	0.75-m	PM
December	3/4	2446768	346	4.33	3.08	MJO	B	0.6-m	AvdP/DJS
December	4/5	2446769	587	6.95	2.87	SAAO	B	0.75-m	PM
December	4/5	2446769	371	4.26	3.06	MJO	B	0.6-m	AvdP/DJS
December	4/5	2446769	544	6.14	3.11	MKO	astb	0.6-m	JMM
December	5/6	2446770	590	6.84	2.71	SAAO	B	0.75-m	PM
December	5/6	2446770	220	3.17	2.34	MJO	B	0.6-m	AvdP/DJS
December	6/7	2446771	395	5.30	2.23	SAAO	B	0.75-m	PM

Table 1 — *continued*

Date		JD	N 40-s	t hr	σ mmag	Obs	Fil	Tel	Obsr
1986									
December	7/8	2446772	581	6.67	2.11	SAAO	B	0.75-m	PM
December	7/8	2446772	444	5.96	2.42	MKO	astb	0.6-m	JMM
December	8/9	2446773	548	6.61	2.27	SAAO	B	0.75-m	PM
December	8/9	2446773	588	6.56	2.82	MKO	astb	0.6-m	JMM
December	9/10	2446774	579	6.64	1.81	MKO	astb	0.6-m	JMM
December	10/11	2446775	502	5.70	1.83	MKO	astb	0.6-m	JMM
December	11/12	2446776	522	5.91	2.53	MKO	astb	0.6-m	JMM
December	14/15	2446779	133	1.45	1.24	MKO	astb	2.2-m	JMM
December	15/16	2446780	333	3.60	2.73	MKO	astb	2.2-m	JMM
December	16/17	2446781	597	6.40	2.62	MKO	astb	0.6-m	JMM
December	17/18	2446782	582	6.19	2.65	MKO	astb	0.6-m	JMM
December	18/19	2446783	533	5.66	2.93	MKO	astb	0.6-m	JMM
December	19/20	2446784	529	5.69	2.23	MKO	astb	0.6-m	JMM
Σ			30876	365.05					
Σ (all years)			47864	579.69					

CTIO = Cerro Tololo Inter-American Observatory
ESO = European Southern Observatory
LO = Lowell Observatory
MDO = McDonald Observatory
MKO = Mauna Kea Observatory
MSSSO = Mount Stromlo and Siding Spring Observatory
MJO = Mount John Observatory
SAAO = South African Astronomical Observatory
WO = The Florence and George Wise Observatory

JCC = J. C. Clemens
MSC = M. S. Cropper
SDK = S. D. Kawaler
SOK = S. O. Kepler
TJK = T. J. Kreidl
DWK = D. W. Kurtz
PM = P. Martinez
JMM = J. M. Matthews
AvdP = A. van der Peet
HS = H. Schneider
JS = J. Seeman
CS = C. Sterken
DJS = D. J. Sullivan
HJW = H. J. Wood
WWW = W. W. Weiss

stars indicate that the amplitude of the oscillation is similar in *U* and *B*; in *V* it is about half that in *U* and *B*. Some of our observations were obtained with two-channel or multi-channel systems to make a similar study of HR 1217. TJK's Lowell Observatory observations were made simultaneously through Johnson *B* and *V* filters. CS's European Southern Observatory observations were made simultaneously through Strömgren *uvby* filters. In Section 4.6 we discuss the amplitude versus bandpass relation for HR 1217 based on these observations. It is now clear that a narrow-band filter in the blue would give the best signal-to-noise ratio for this star. We chose in this study to use the Johnson *B* filter because its wide availability assured that all potential observers would have the correct filter. The observations by JMM obtained at Mauna Kea Observatory were made through an 'asteroid *b*' filter, essentially the same as a Johnson *B* filter.

The integration times used in the observations varied between observatories. Our original intention was to gather all of the data using continuous 10-s integrations; some of the equipment did not easily allow for that, however. Observations made at SAAO, MSSSO, LO, CTIO, MDO and MJO (see Table 1 for an explanation of these acronyms) were made using

continuous 10-s integrations. Observations at ESO by HS/WWW used 16-s integrations which were recorded at alternating 24- and 22-s intervals. Observations at ESO by CS through *uvby* filters used 12-s integrations. Observations at MKO used 10-s integrations obtained at 12.5-s intervals.

All of these observations were averaged to 40-s integrations, or to an integration time as close to that as possible. Hence the 12-s integrations were averaged to 36-s; the 12.5-s integrations to 37.5-s; alternating 24- and 22-s data-capture-time 16-s integrations to 46-s. The net result of this is that the 36- and 37.5-s integrations are weighted slightly more heavily (since the weighting is by number of data points) in the frequency analysis than the 40-s integrations, and the 46-s integrations slightly less heavily. Given the size of our dataset and the rotational phase coverage of the data, we see no reason why this slightly unequal weighting should systematically affect our analysis. Our technique of frequency analysis easily allows for the re-weighting of the data, but other techniques with which our analysis may be compared may not easily allow for re-weighting; we felt it was important to keep the analysis straightforward for the benefit of those who may re-analyse the data which are now in the public domain.

All of the observations were corrected for dead-time losses, sky background and mean extinction. The times were corrected to Heliocentric Julian Date to an accuracy of 10^{-5} d (i.e. ≈ 1 s). Because we have several cases of simultaneous data obtained from different observatories, it was possible to cross-check these overlapping data. In general, the oscillations in the overlapping data agreed to $\pm 1\sigma$ in phase. In the worst case, however, on JD2446769 where we have 2.6 hr of overlapping data from MKO and MJO, there is a phase shift between the two datasets of 0.62 ± 0.11 rad; this corresponds to a time shift of 36 ± 6 s. We cannot tell *a posteriori* whether this shift is real, due possibly to a clock error, or whether the shift is just statistical and our internal error estimate in phase is unrealistically low. The latter seems possible since overlapping data from MKO and MJO must, of necessity, be obtained at high hour angle at both observatories. If the shift is real, it will cause some very small systematic errors in the frequency analysis due to a small amount of phase smearing.

All of the data were filtered for low-frequency sky transparency variations. These variations occur on even the best photometric nights and range from < 1 mmag for excellent nights at good sites up a few hundredths of a mag on usable, but not outstanding, photometric nights. It is important to remove these peaks from the data, especially for the larger-amplitude peaks, because the window pattern generally has relatively small bumps on it even fairly far from the central frequency. A relatively small bump out on the wing of a low-frequency sky transparency peak with an amplitude of 10 mmag might perturb the signal we are interested in. Another reason for filtering the low-frequency sky transparency noise is that we fit the determined frequencies to the data with a least-squares routine. This routine is predicated on the assumption of white noise; the error calculations make use of the total variance in the data which would give overestimates of the errors if the low-frequency noise were not filtered.

Our filtering procedure removed the low-frequency peaks in the amplitude spectrum of each night of data for frequencies less than about 0.6 mHz (periods greater than 0.5 hr) by prewhitening them in the time domain. Thus we only filtered peaks which were clearly separated in the amplitude spectrum from the pulsation frequencies in HR 1217 (near 2.7 mHz). On some nights the low-frequency peaks were not clearly separated from the pulsation ferquencies. In general, we took that to be evidence of a non-photometric night and rejected the data from further analysis. An exception to this was for very short data strings where the width of the peaks in the amplitude spectum caused the low frequencies and high frequencies to interfere with each other. We only retained such data when the low-frequency peak appeared to be due to a slight variation in the extinction coefficient with respect to the mean coefficient used in the initial reduction.

3 The time of amplitude maximum

From the previous work of Kurtz (1982), Kurtz & Seeman (1983) and Kurtz, Schneider & Weiss (1985) it is clear that the principal frequencies of HR 1217 are amplitude modulated with the rotation period, or something very close to it. To examine this amplitude modulation more closely, we fitted by least-squares the central principal frequency (determined in the frequency analysis in Section 4.4 below) of $\nu = 2.68760$ mHz to sections of the data 0.01723-d long (i.e. 24.8 min ≈ four pulsation cycles) for the JD2446738–2446784 data listed in Table 1.

This gave us 711 measures of the pulsation amplitude as a function of rotation phase which are plotted in Fig. 1. We have used the rotation period given by Kurtz & Marang (1987) of $P_{\rm rot} = 12.4572$ d. The time of pulsation maximum was determined by performing a frequency analysis on the data shown in Fig. 1. That gave $t_0 = \text{JD}2446744.15 \pm 0.10$, which is intermediate between the time of mean light minimum ($t_0 = \text{JD}2446744.54 \pm 0.09$) and the time of magnetic maximum ($t_0 = \text{JD}2446743.54 \pm 0.38$) given by Kurtz & Marang (1987). Hence t_0(pulsation maximum) − t_0(mean light minimum) = -0.39 ± 0.13 d = -0.031 ± 0.010 rotation periods, and t_0(pulsation maximum) − t_0(magnetic maximum) = 0.61 ± 0.39 d = 0.05 ± 0.03 rotation periods. If there are no systematic errors affecting this analysis, then the time of pulsation maximum is not significantly different from the time of magnetic maximum, but it is significantly different from the time of mean light minimum. Assuming that HR 1217 is an oblique pulsator, we conclude from this that the pulsation axis is probably aligned with the magnetic axis and that the abundance distribution which gives rise to the mean light variations is not concentric with the magnetic and pulsation axes. This is consistent with Bonsack's (1979) conclusions from a study of the line-blocking coefficients.

Amplitude modulation on time-scales much shorter than the rotation period due to the beating of the principal frequencies causes the large scatter in the amplitudes plotted in Fig. 1. Still, the rotational amplitude modulation is clear in the diagram from the upper envelope of

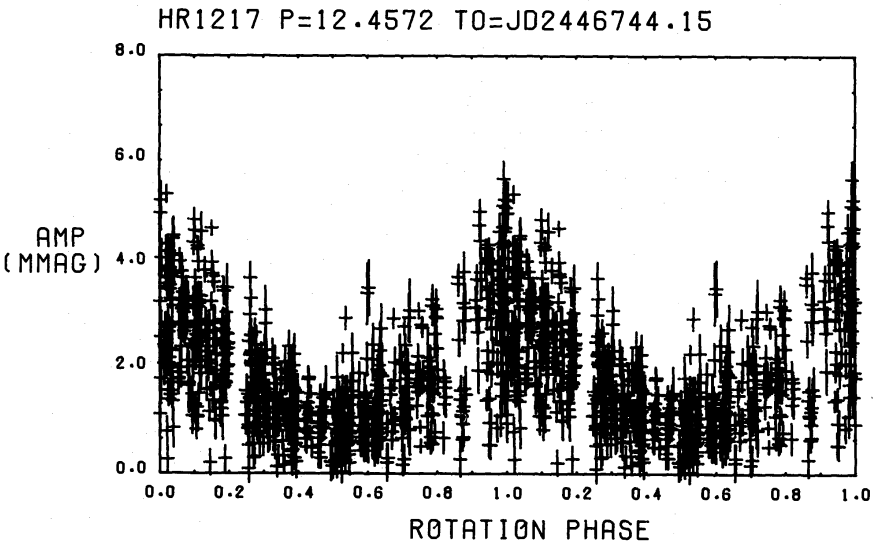

Figure 1. Pulsation amplitude versus rotational phase. The pulsation amplitude has been calculated by fitting the single frequency $\nu = 2.68760$ mHz to sections of the data four pulsation cycles (24.8 min) long. The rotational period used is $P_{\rm rot} = 12.4572$ d determined by Kurtz & Marang (1987). The time of amplitude maximum was determined by performing a Fourier frequency analysis on the data plotted in this diagram. That time is consistent with the time of magnetic maximum and appears to differ from the time of mean light minimum. The large scatter at all phases is partly due to the beating of the principal frequencies which are unresolved over four pulsation cycles. The upper envelope of the points shows the sinusoidal amplitude modulation expected of an oblique pulsator.

the points. Fig. 1 also shows that our data give very good rotational phase coverage, an important point when we search for rotational sidelobes to the principal frequencies in the frequency analyses presented in Section 4.

Kurtz (1982) showed that the time of pulsation amplitude maximum and magnetic maximum coincided within an estimated error of ±0.3 d at JD2444576.8 and JD2444638.9. From this he concluded that if the amplitude modulation of the pulsation were due to excited m-modes, then the constant $C_{n,l}$ in the rotational splitting relation

$$\nu_m = \nu_0 - m(1 - C_{n,l})\,\nu_{\rm rot} \tag{2}$$

(Ledoux 1951) must be $C_{n,l} \leq 0.014$ at the 3σ confidence level. From the data in Fig. 1 we have determined that amplitude maximum still coincides with magnetic maximum within ±0.4 d at JD2446781.5. Hence we can now place an upper limit on $C_{n,l}$ of $C_{n,l} \leq 0.0006$ at the 3σ confidence level. This is much less than the expected value of $C_{n,l} \approx 0.01$ (Shibahashi & Saio 1985) and indicates that the amplitude modulation is not due to the excitation of m-modes. In addition, the coincidence of pulsation maximum and magnetic maximum is purely accidental unless $C_{n,l} = 0$ exactly; this also argues strongly that the amplitude modulation is not due to the excitation of m-modes. This coincidence of pulsation maximum and magnetic maximum is also seen in the rapidly oscillating Ap star HR 3831 (Kurtz & Shibahashi 1986).

4 Frequency analysis

Frequency analyses of various combinations of the B data listed in Table 1 were performed using a fast algorithm (Kurtz 1985) based on Deeming's (1975) Discrete Fourier Transform. We also employed an interpolation technique (O'Donoghue 1981; O'Donoghue & Warner 1982) which significantly reduces computing time. Each of the following sections demonstrate important features of the frequency spectrum of HR 1217.

Section 4.1 shows the frequency analysis of a 16-hr dataset centred on the time of amplitude maximum; this shows the presence of six principal frequencies. Section 4.2 shows the frequency analysis of a dataset spanning a little over one rotation cycle; this shows the rotational sidelobes of the principal frequencies. Section 4.3 shows a frequency analysis of data obtained from a single site over a time-span of 5 weeks when the weather was 67 per cent photometric; this shows that the frequency spectrum cannot be solved with data from a single site and that the multi-site campaign was essential. Section 4.4 shows a frequency analysis of all of the B data from all sites obtained during the time-span JD2446738–2446784; this shows the principal frequencies and rotational sidelobes to higher accuracy than in Section 4.2 and it also shows secondary frequencies which indicate that some of the principal frequencies are amplitude modulated on a time-scale of the order of the length of the dataset. Section 4.5 describes the failure of a frequency analysis of all of the B data listed in Table 1 spanning 5 yr. Section 4.6 discusses the amplitudes and phases of the principal frequencies as a function of the filter for the multi-colour observations obtained at LO and ESO.

4.1 A 16-HR DATASET AT AMPLITUDE MAXIMUM

The first step in our analysis was to examine data strings near the time of amplitude maximum in a manner similar to the analysis of Kurtz & Seeman (1983). From the time of amplitude maximum determined in Section 3 and the rotation period given by Kurtz & Marang (1987) we have a pulsation ephemeris of

$$\begin{aligned} \text{HJD(amplitude maximum)} = 2446744.15 &+ 12.4572\,E \\ \pm 0.10 \quad &\pm 0.0003 \end{aligned} \tag{3}$$

which indicates that pulsation maxima are expected at JD2446744.15 and JD2446769.06 – times when we have long data strings from more than one site (see Table 1).

We analysed several combinations of continuous, or nearly continuous data, all of which gave similar results. We illustrate the results in Fig. 2, which is an amplitude spectrum of the data obtained at MSSSO and SAAO on JD2446744. These data have a time distribution of t(MSSSO) = 6.81 hr, gap = 1.61 hr, t(SAAO) = 7.31 hr, for a total time-span of 15.73 hr starting at HJD2446743.93191 and ending at HJD2446744.58751 – nicely spanning the time of amplitude maximum.

Six frequencies stand out above the noise in Fig. 2 and are labelled in order of increasing frequency. They are (the values in parentheses are those derived by Kurtz & Seeman from their 1981 data) $\nu_1 = 2.627$ mHz (2.620), $\nu_2 = 2.654$ mHz (2.653), $\nu_3 = 2.684$ mHz (2.688), $\nu_4 = 2.725$ mHz (2.721), $\nu_5 = 2.751$ mHz (2.756) and $\nu_6 = 2.803$ mHz (2.794). The full width at half-maximum (FWHM) of the peaks in Fig. 1 is 0.004 mHz so the values we find for ν_1 to ν_6 agree well with those of Kurtz & Seeman obtained 5 yr previously. Hereafter, we shall refer to these six frequencies as the principal frequencies.

We find that for short data strings like those of Kurtz & Seeman and that used to produce the amplitude spectrum in Fig. 2, the relative amplitudes derived for ν_1 to ν_6 are highly variable. This is due to incomplete sampling and the beating between those frequencies, as well as longer-term amplitude modulation of some of them (see Section 4.4). It is not safe, therefore,

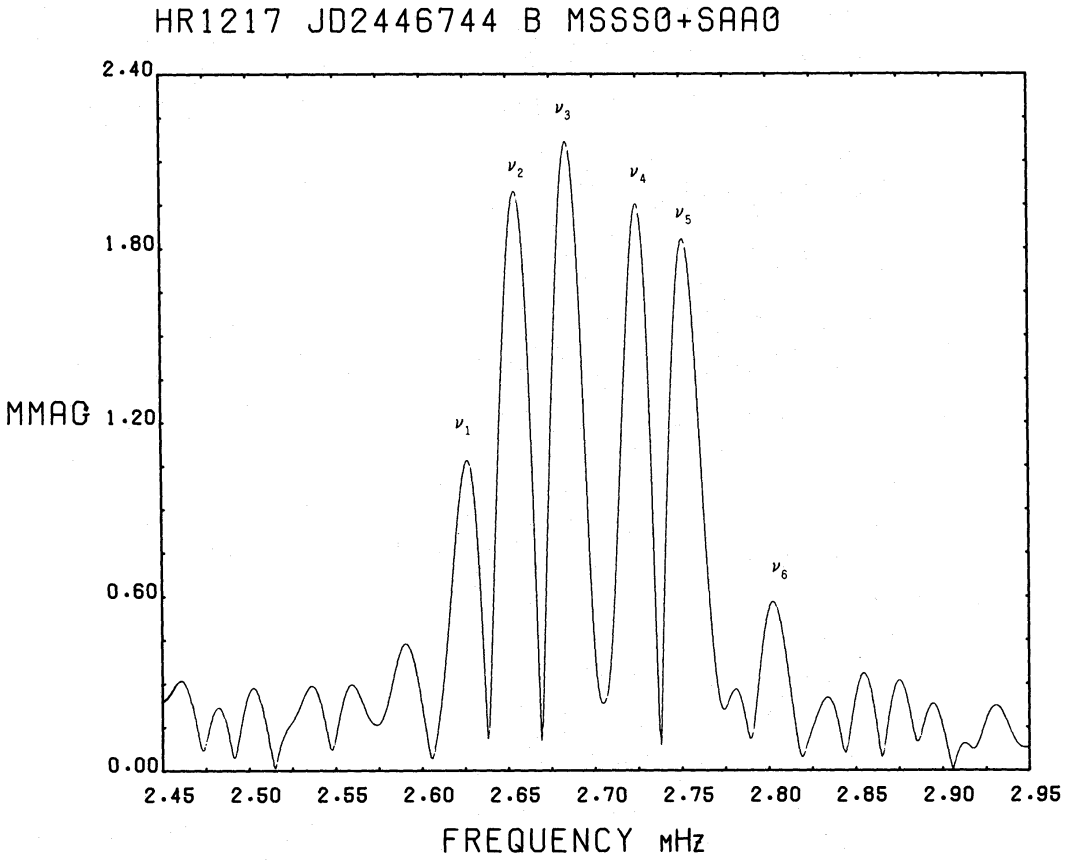

Figure 2. An amplitude spectrum of 15.73 hr of nearly continuous data obtained at SAAO and MSSSO. The midpoint of the light curve occurs at JD2446744.26; amplitude maximum occurs at JD2446744.15. The six frequencies labelled are the same as those determined from much more extensive data and also the same as those determined by Kurtz & Seeman (1983).

to attempt any mode assignments based on the relative amplitudes of the frequencies determined from short data strings.

4.2 THE JD2446739–2446753 MULTI-SITE DATA

As the next step in our analysis we analysed the *B* data obtained from JD2446738–2446753 from all observing sites. This dataset spans 15.61197 d = 374.69 hr, during which observations were obtained for 140 hr, giving a 37 per cent duty cycle. All of the amplitude spectra which we show in this paper are restricted to the range $2.45\,\text{mHz} \leq \nu \leq 2.95\,\text{mHz}$. Kurtz (1982) showed that all of the oscillation frequencies of HR 1217 lie well within this range and we confirm that with the new data. This frequency range adequately shows all of the oscillation frequencies and a section of noise on both the high- and low-frequency sides of them.

Fig. 3 is the spectral window for this dataset. It was created by sampling a noise-free sinusoid of $\nu = 2.68760\,\text{mHz}$ and $A = 1.1\,\text{mmag}$ at the same times as the actual data points. The 1, 2 and $3\,\text{d}^{-1}$ aliases have amplitudes 48, 23 and 13 per cent of the amplitude of the main peak. It is the $3\,\text{d}^{-1}$ aliases which plague the frequency analysis of data obtained from a single observing site because the principal frequencies are separated by about $34\,\mu\text{Hz}$; $3\,\text{d}^{-1} = 34.7\,\mu\text{Hz}$. Fig. 3 demonstrates that these aliases are essentially no problem in the analysis of this dataset.

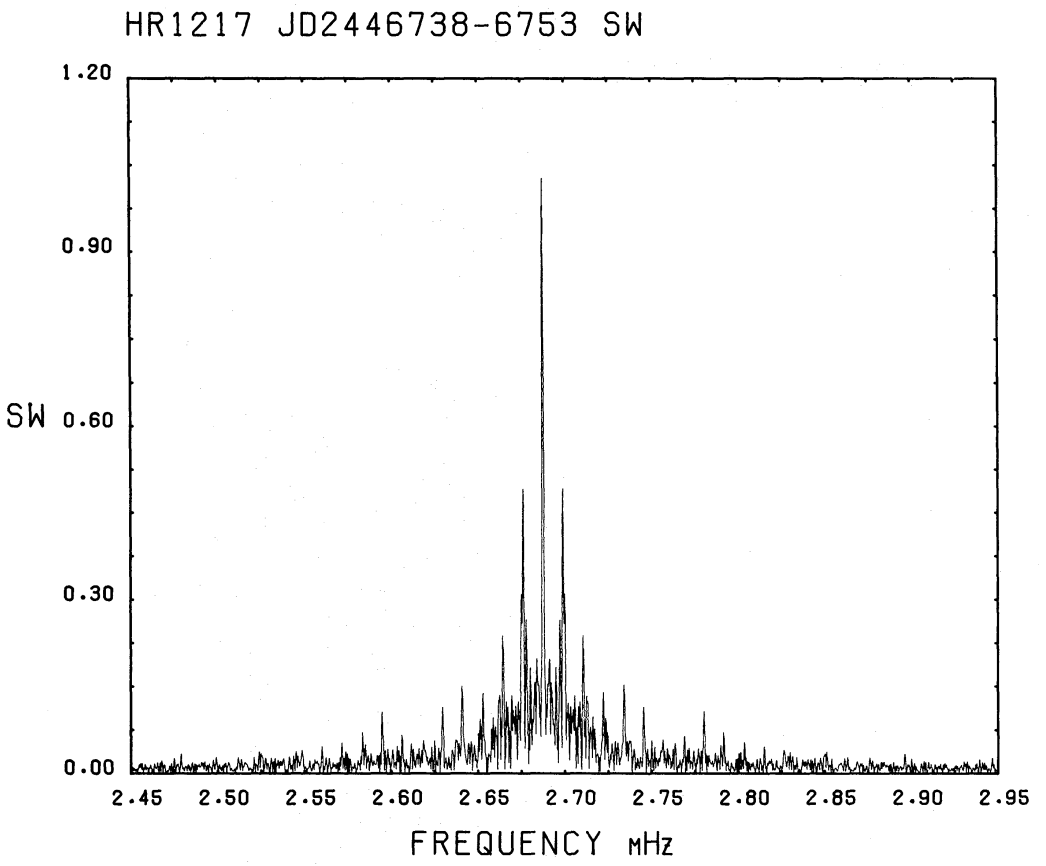

Figure 3. The spectral window of the JD2446738–2446753 *B* multi-site data. The window pattern was produced by sampling a noise-free sinusoid of $\nu = 2.68760\,\text{mHz}$ and $A = 1.1\,\text{mmag}$ at the same times as the actual data points. The 1, 2 and $3\,\text{d}^{-1}$ aliases have amplitudes 48, 23 and 13 per cent of the amplitude of the main peak, respectively.

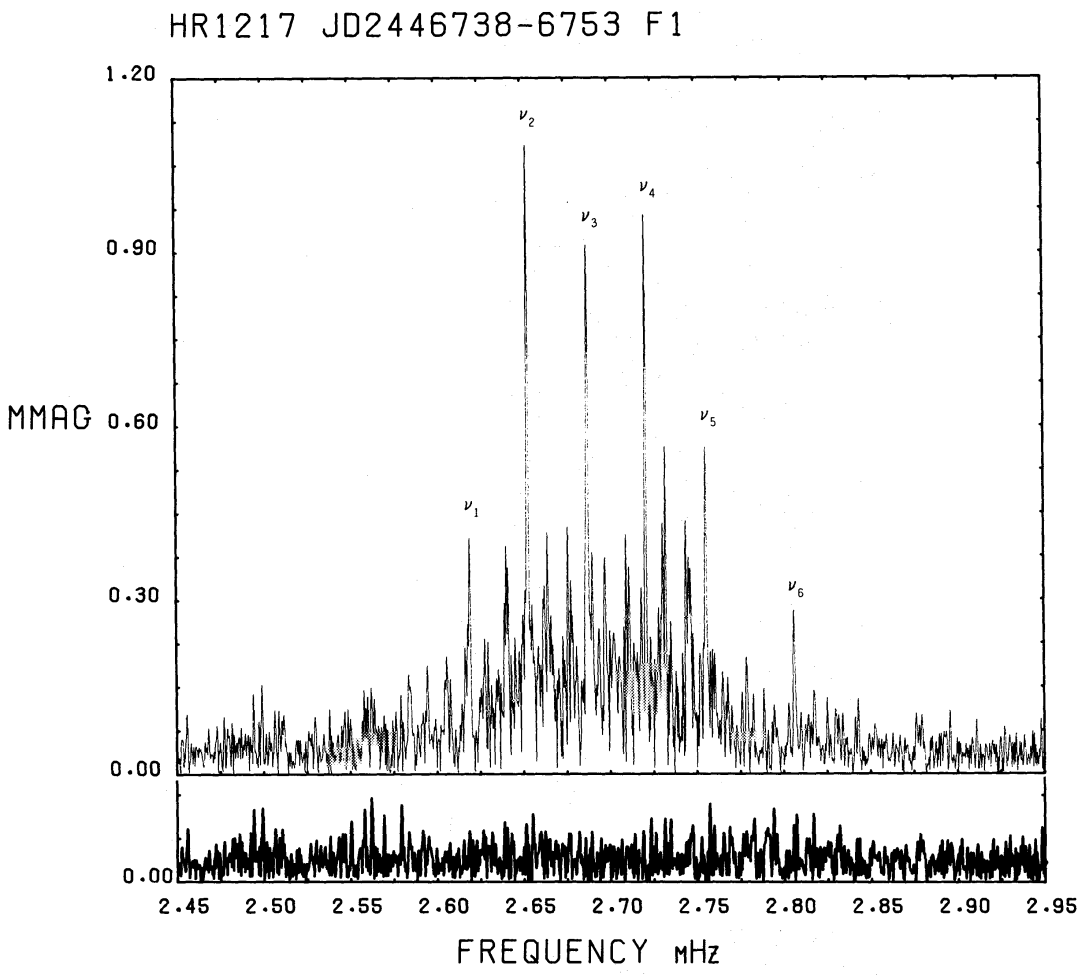

Figure 4. The amplitude spectrum of the JD 2446738–2446753 *B* multi-site data. The principal frequencies ν_1 to ν_6 are labelled. After prewhitening by ν_1 to ν_6 and the rotational sidelobes of ν_2, ν_3, ν_4 and ν_5, nothing is left in the amplitude spectrum of the residuals except noise, which is shown in the bottom panel on the same scale.

Fig. 4 shows an amplitude spectrum for this dataset with the principal frequencies ν_1 to ν_6 labelled in order of increasing frequency. From the spectral window we know that the $3\,d^{-1}$ aliases are no problem. The 1 and $2\,d^{-1}$ may appear to cause some confusion between ν_1 and ν_2 and between ν_4 and ν_5, but this confusion is merely cosmetic and is easily overcome (by prewhitening or by an examination of the window pattern). The three frequencies of highest amplitude are unambiguous in Fig. 4: $\nu_2 = 2.6530$ mHz, $\nu_3 = 2.6875$ mHz and $\nu_4 = 2.7210$ mHz.

We fitted ν_2, ν_3 and ν_4 to the data simultaneously by least-squares and then removed them from the data in the time domain (a process we shall call prewhitening). In an amplitude spectrum of the residuals we then selected the next highest peaks. We continued this process of fitting all previously determined frequencies to the data simultaneously by least-squares, then prewhitening the data and examining the amplitude spectrum of the residuals until we could no longer select peaks unambiguously from the amplitude spectrum. This resulted in 14 frequencies which are given in Table 2 along with their amplitudes and phases determined from a simultaneous least-squares fit. These frequencies are the six principal frequencies and the rotational sidelobes of the four principal frequencies of highest amplitude. The error quoted for the frequencies is $1/4\,\Delta T$ which is approximately the FWHM of the peaks in the amplitude spectrum. After prewhitening these 14 frequencies nothing was left in the amplitude

Table 2. A least-squares fit of 14 derived frequencies to the JD2446738–2446753 multi-site *B* data.

name	frequency mHz ±0.0002	amp mmag ±0.026	phase radians
ν_1	2.6195	0.272	-1.79±0.09
$\nu_2-\nu_{rot}$	2.6520	0.384	-2.41±0.07
ν_2	2.6530	1.076	-2.38±0.02
$\nu_2+\nu_{rot}$	2.6541	0.292	-2.58±0.09
$\nu_3-\nu_{rot}$	2.6865	0.506	-2.24±0.05
ν_3	2.6875	0.963	-2.65±0.03
$\nu_3+\nu_{rot}$	2.6885	0.350	-2.37±0.07
$\nu_4-\nu_{rot}$	2.7202	0.266	0.41±0.10
ν_4	2.7210	1.174	0.76±0.02
$\nu_4+\nu_{rot}$	2.7220	0.409	0.82±0.06
$\nu_5-\nu_{rot}$	2.7545	0.285	2.21±0.09
ν_5	2.7554	0.466	2.41±0.06
$\nu_5+\nu_{rot}$	2.7564	0.232	2.36±0.11
ν_6	2.8062	0.243	0.89±0.10

σ=1.872 mmag

$\nu_2-(\nu_2-\nu_{rot})=\nu_{rot}$=1.0±0.2 μHz
$(\nu_2+\nu_{rot})-\nu_2=\nu_{rot}$=1.1±0.2 μHz
$\nu_3-(\nu_3-\nu_{rot})=\nu_{rot}$=1.0±0.2 μHz
$(\nu_3+\nu_{rot})-\nu_3=\nu_{rot}$=1.0±0.2 μHz
$\nu_4-(\nu_4-\nu_{rot})=\nu_{rot}$=0.8±0.2 μHz
$(\nu_4+\nu_{rot})-\nu_4=\nu_{rot}$=1.0±0.2 μHz
$\nu_5-(\nu_5-\nu_{rot})=\nu_{rot}$=0.9±0.2 μHz
$(\nu_5+\nu_{rot})-\nu_5=\nu_{rot}$=1.0±0.2 μHz

$\langle\nu_{rot}\rangle$=0.98±0.09 μHz
ν_{rot}(Kurtz & Marang 1987)=0.92911±0.00002 μHz

$\nu_2-\nu_1$=33.5±0.3 μHz
$\nu_3-\nu_2$=34.5±0.3 μHz
$\nu_4-\nu_3$=33.5±0.3 μHz
$\nu_5-\nu_4$=34.4±0.3 μHz
$\nu_6-\nu_5$=50.8±0.3 μHz

$\Delta_1=[(\nu_4-\nu_3)+(\nu_2-\nu_1)]/2$=33.5±0.3 μHz
$\Delta_2=[(\nu_5-\nu_4)+(\nu_3-\nu_2)]/2$=34.5±0.3 mHz

$(\nu_6-\nu_5)/\Delta_1$=1.52±0.02
$(\nu_6-\nu_5)/\Delta_2$=1.47±0.02

Note: the phase is determined from t_0 = JD2446744.15.

spectrum of the residuals but noise which is shown in the lower panel of Fig. 4. Fig. 5 is a schematic amplitude spectrum which illustrates the results of this analysis given in Table 2.

The average separation of the rotational sidelobes from the principal frequencies is given in Table 2 and is within 1σ of the rotation frequency derived by Kurtz & Marang (1987). That, combined with the coincidence of amplitude maximum and magnetic maximum shown in Fig. 1 for the 1986 data and determined by Kurtz (1982) for the 1981 data, argues that the rotational sidelobes are separated from the principal frequencies by *exactly* the rotation frequency. Assuming this to be true, we fitted the principal frequencies plus their rotational sidelobes (calculated using the rotational frequency given by Kurtz & Marang) to the JD2446738–2446753 data by least-squares with the results shown in Table 3. The rotational sidelobes for ν_1 and ν_6 have amplitudes less than the highest noise peaks shown the lower panel of Fig. 4 and hence are rejected and marked as such in Table 3.

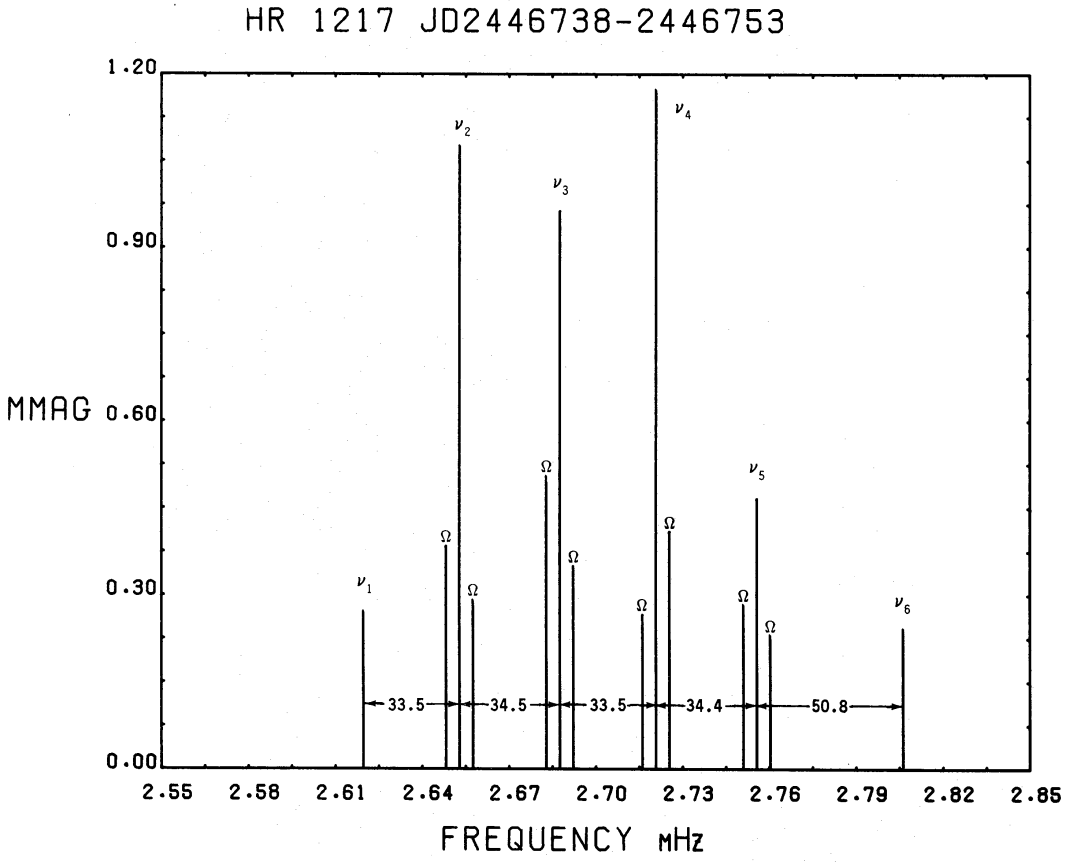

Figure 5. A schematic amplitude spectrum of the frequencies derived from the JD2446738–2446753 *B* data. A least-squares fit of these frequencies to the data is given in Table 2. The spacing of the principal frequencies is to scale; the separations are in μHz and are taken from Table 2. The rotational sidelobes are marked Ω; their separations from the principal frequencies have been exaggerated for clarity.

There are several important features to Tables 2 and 3 which should be noted and will be discussed in Section 5:

(i) The frequency spacing of the principal frequencies is not uniform; $\nu_2-\nu_1=\nu_4-\nu_3\equiv\Delta_1$ and $\nu_3-\nu_2=\nu_5-\nu_4\equiv\Delta_2$, where $\Delta_1<\Delta_2$ (see Fig. 5). This last result is only significant at the 2.5σ confidence level, but we will show in the next section that it holds true at the 13σ confidence level for a much larger dataset where the frequencies can be determined to higher accuracy. This is the inequality which was noted by Shibahashi & Saio (1985) in Kurtz & Seeman's (1983) analysis of HR 1217 which, in part, led them to suggest that the principal frequencies are due to alternating even and odd *l*-modes.

(ii) In the notation of the oblique pulsator model (Kurtz & Shibahashi 1986), for each frequency triplet let $A^{(l)}_{-1}$ be the amplitude of the low frequency rotational sidelobe, $A^{(l)}_{+1}$ be the amplitude of the high frequency rotational sidelobe and A_0 be the amplitude of the principal frequency. The parameter $x\equiv(A^{(l)}_{+1}+A^{(l)}_{-1})/A^{(l)}_0$ is then a function of the pulsation mode associated with each principal frequency. From Table 3 we see that $x(\nu_2)=x(\nu_4)\equiv x_1$ and $x(\nu_3)=x(\nu_5)\equiv x_2$, where $x_1\neq x_2$.

(iii) The phases of each principal frequency and its rotational sidelobes are equal at the time of magnetic maximum. This tells us that all of the principal frequencies are at amplitude maximum at the time of magnetic maximum and are at amplitude minimum at the time of magnetic minimum.

Table 3. A least-squares fit of the six derived principal frequencies and their calculated rotational sidelobes to the JD2446738–2446753 multi-site *B* data.

name	frequency mHz	amp mmag ±0.025	phase radians	$x=A_{+1}+A_{-1}/A_0$
$\nu_1-\nu_{rot}$	2.6186	0.092	-1.67±0.27 reject	
ν_1	2.6195	0.292	-1.79±0.09	
$\nu_1+\nu_{rot}$	2.6204	0.073	-1.47±0.34 reject	
$\nu_2-\nu_{rot}$	2.6521	0.397	-2.49±0.06	
ν_2	2.6530	1.053	-2.39±0.03	0.64±0.04
$\nu_2+\nu_{rot}$	2.6539	0.278	-2.32±0.09	
$\nu_3-\nu_{rot}$	2.6866	0.511	-2.43±0.05	
ν_3	2.6875	0.942	-2.64±0.03	0.92±0.04
$\nu_3+\nu_{rot}$	2.6884	0.359	-2.28±0.07	
$\nu_4-\nu_{rot}$	2.7201	0.262	0.49±0.10	
ν_4	2.7210	1.178	0.72±0.02	0.57±0.09
$\nu_4+\nu_{rot}$	2.7219	0.411	0.96±0.06	
$\nu_5-\nu_{rot}$	2.7545	0.282	2.17±0.09	
ν_5	2.7554	0.471	2.39±0.05	1.08±0.09
$\nu_5+\nu_{rot}$	2.7563	0.226	2.48±0.11	
$\nu_6-\nu_{rot}$	2.8053	0.098	-2.17±0.25 reject	
ν_6	2.8062	0.223	0.87±0.11	
$\nu_6+\nu_{rot}$	2.8071	0.115	-0.34±0.22 reject	

σ=1.868 mmag

Note: the phase is determined from t_0 = JD2446744.15.

(iv) The separation $\nu_6-\nu_5$ is about 1.5 times the other separations of the principal frequencies.

4.3 THE JD2446739–2446773 SAAO DATA

Fig. 6 shows an amplitude spectrum of the data obtained only at SAAO from JD2446739–2446773. These data cover 171.41 hr of observations obtained over 34 d for a 21 per cent duty cycle. HR 1217 is only observable from SAAO for about 7.5 hr per night; the weather over that 34-d time-span was about 67 per cent photometric. While this is clearly as good a dataset as is likely to be obtained from a single observing site, it is also inadequate for decoding the frequency spectrum of HR 1217. The frequency of highest amplitude in Fig. 5 is one of the principal frequencies of HR 1217, but the next two highest peaks (which remain the same after prewhitening by the highest peak) are both $1\,d^{-1}$ aliases of the true principal frequencies. Thus Fig. 5 graphically demonstrates the need for multi-site observations.

4.4 THE JD2446738–2446784 MULTI-SITE DATA

As the next step in our analysis we analysed all of the *B* data listed in Table 1 obtained from JD2446738–2446784 (hereafter 'the data', unless otherwise specified). They constitute 27 691 data points (≈ 40-s integrations) gathered during 324 hr of observations over a 46-d

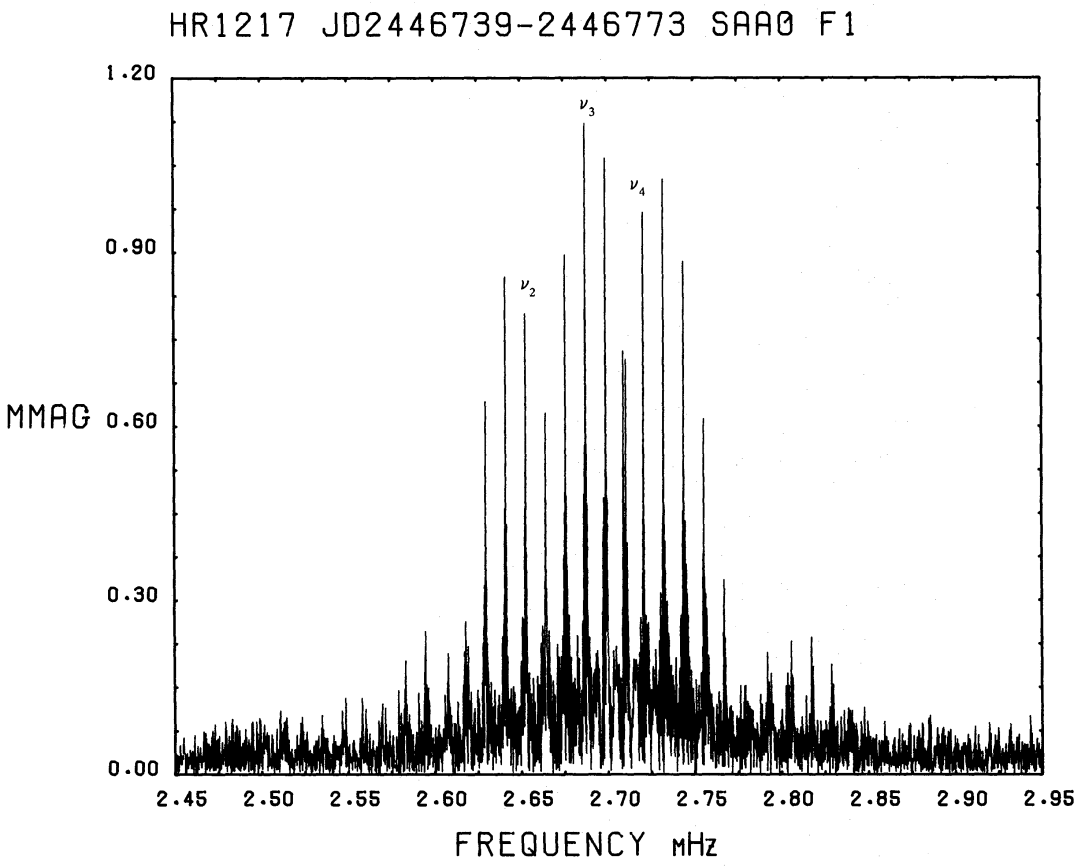

Figure 6. An amplitude spectrum of 171 hr of data obtained from SAAO only. The data have a 21 per cent duty cycle and were obtained during a 34-d time-span in which the weather was 67 per cent photometric. These data therefore are close to the best which can be obtained from a single observing site. The alias problem is insurmountable. The three frequencies of highest amplitude found in the analysis of the multi-site data are marked. Prewhitening by ν_3 still leads to incorrect selections for ν_2 and ν_4. The comparison of this diagram with Fig. 8 provides the justification for the multi-site observing campaign.

time-span. Our duty cycle is hence about 29 per cent for these data and they span almost four rotation cycles. The longitudes of the observatories from which the data were obtained are well-spread (the bulk of the data come from SAAO and MKO which are nearly antipodal) and the data are well-distributed over the rotation cycle (see Fig. 1).

Fig. 7 is the spectral window of the data. It was created by sampling a noise-free sinudoid of $\nu = 2.68760$ mHz and $A = 1.1$ mmag at the same times as the actual data points. The 1, 2 and $3\,d^{-1}$ aliases have amplitudes of 35, 38 and 12 per cent of the amplitude of the main peak. As was the case for the JD2446738–2446753 data analysed in Section 4.2, the aliases in Fig. 7 cause mostly minor cosmetic blemishes which are overcome by prewhitening.

Fig. 8 shows an amplitude spectrum of the data with the frequencies ν_1 to ν_6 labelled. The three frequencies of highest amplitude are unambiguous: $\nu_2 = 2.65294$ mHz, $\nu_3 = 2.68760$ mHz and $\nu_4 = 2.72085$ mHz. Fig. 9 shows the amplitude spectrum of the residuals after prewhitening the data by ν_2, ν_3 and ν_4 (where the amplitudes and phases of those frequencies were determined by fitting them simultaneously to the data by least-squares). The two highest amplitude peaks here are rotational sidelobes of ν_3 at $\nu_3 - \nu_{rot}$ and $\nu_3 + \nu_{rot}$; ν_5 and ν_6 are also labelled. We continued this process of fitting all previously determined frequencies to the data simultaneously by least-squares and then prewhitening the data and examining the amplitude spectrum of the residuals until we could no longer select peaks unambiguously from the amplitude spectrum. This resulted in 17 frequencies which are given

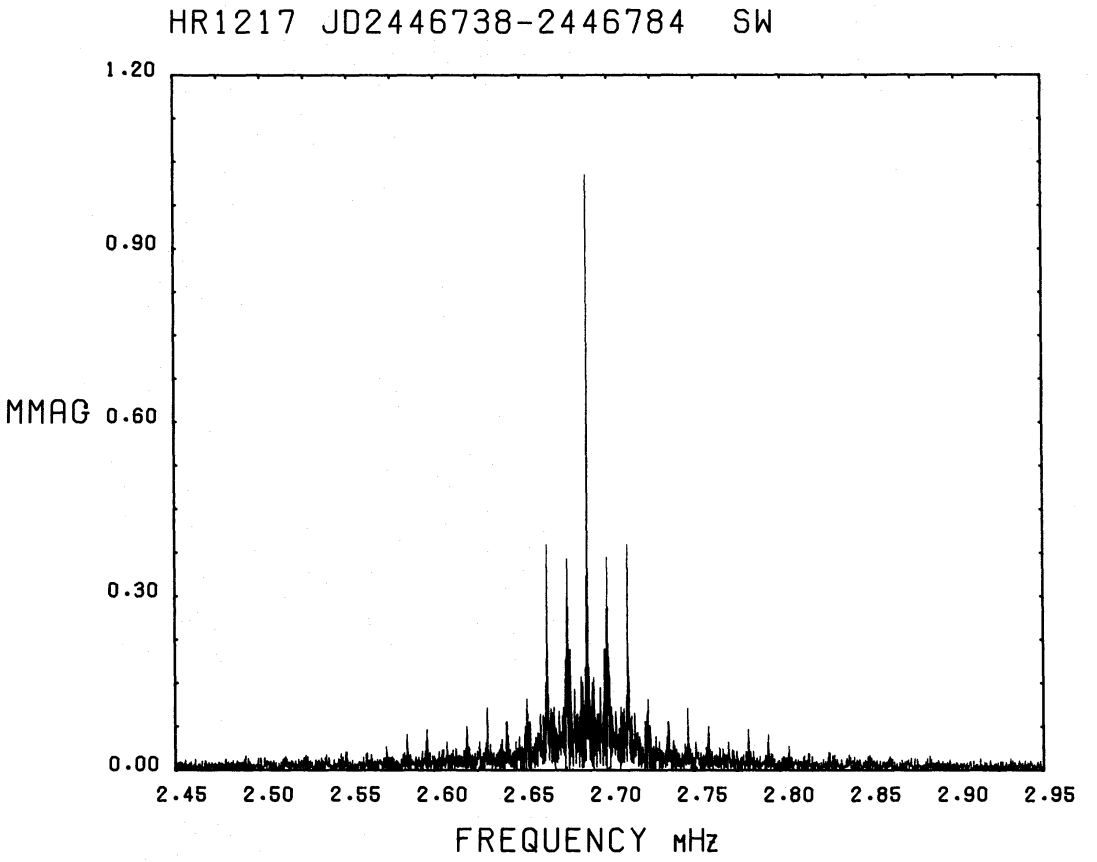

Figure 7. The spectral window of the JD2446738–2446784 *B* multi-site data. The window pattern was produced by sampling a noise-free sinusoid of $\nu = 2.68760$ mHz and $A = 1.1$ mmag at the same time as the actual data points. The 1 and 2 d^{-1} aliases have amplitudes 37 per cent of the amplitude of the main peak and the 3 d^{-1} aliases have amplitudes 12 per cent of the amplitude of the main peak.

in Table 4 along with their amplitudes and phases determined from a simultaneous least-squares fit. The error quoted for the frequencies is $1/4\Delta T$, which is approximately the FWHM of the peaks in the amplitude spectrum. After prewhitening these 17 frequencies the residuals still show significant amplitude in the frequency range of ν_1 to ν_6 with peaks around 0.20 mmag (the highest peaks in the noise can be seen in Figs 8 and 9 to be 0.08 mmag). Hence our frequency analysis is not complete. This, plus the fact that some of the frequencies we have determined are not completely resolved, leads us to the error estimate we have given for the frequencies. In the absence of any resolution problems, the centroid of the peaks in the amplitude spectrum, and hence the frequencies, can be determined to much higher accuracy than this.

The basic pattern of the frequencies in Table 4 is the same as that found for the JD2446738–2446753 data in Section 4.2. There are the six principal frequencies with some of their rotational sidelobes, but now with additional smaller-amplitude frequencies very close to the principal frequencies (labelled with 'p' or 'm' appended to the subscript of the principal frequency to which they are nearest; 'p', plus, for slightly higher frequency, 'm', minus, for slightly lower) which we will refer to as the secondary frequencies. The separations between the principal frequencies and secondary frequencies are generally in the range 0.20–0.30 μHz; one cycle over the 46-d time-span of the dataset is equivalent to a frequency of 0.25 μHz. The secondary frequencies therefore tell us that the principal frequencies are amplitude modulated on approximately the time-scale of the dataset. (On the shorter time-scale of the dataset

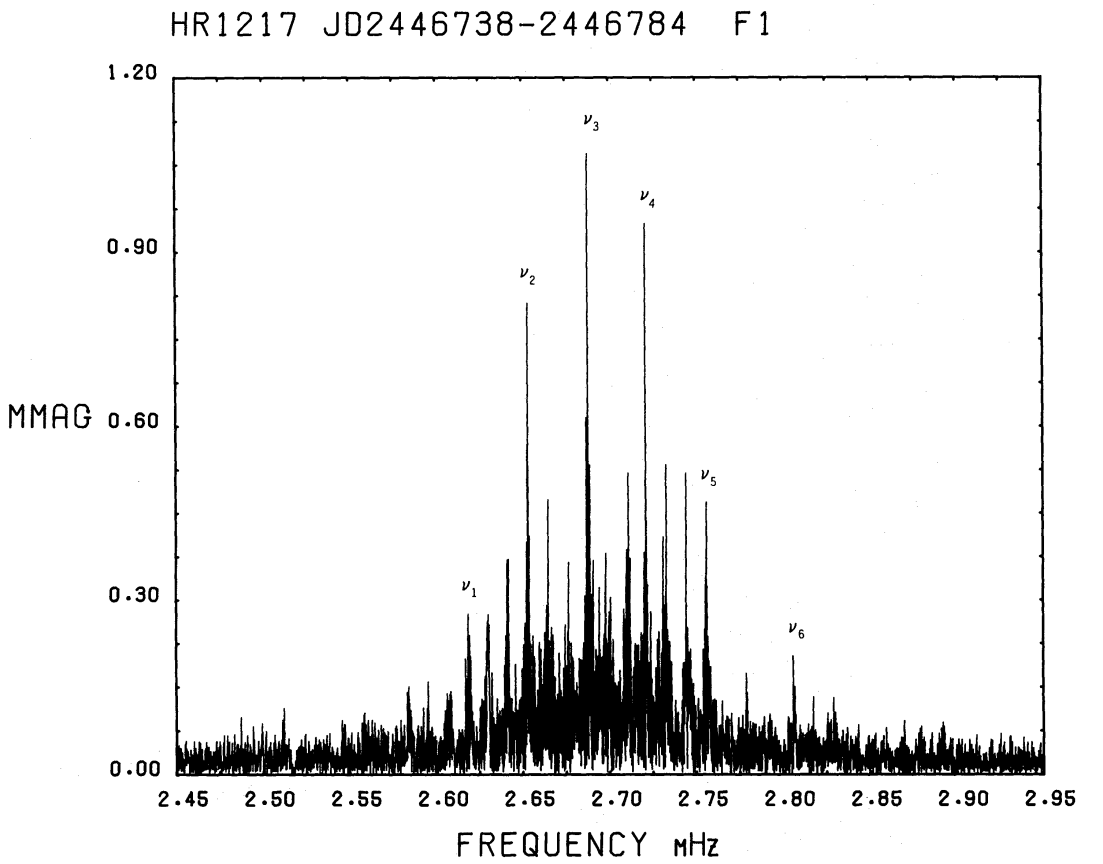

Figure 8. The amplitude spectrum of the JD2446738–2446784 *B* multi-site data. The principal frequencies ν_1 to ν_6 are labelled.

analysed in Section 4.2, the secondary freuqencies are not resolved, and hence did not appear in that analysis – except in their effect on the relative amplitudes of the principal frequencies.)

The separation of the principal frequencies and secondary frequencies means they beat with respect to each other very nearly once over the 46-d time-span of the dataset. That is a time-scale of variation which conceivably might be produced by systematic effects in the data acquisition, so we made some tests to see whether the secondary frequencies are artefacts of our analysis.

As a first step we fitted ν_1 to ν_6 to the data along with their first- and second-order rotational sidelobes calculated using the rotational frequency given by Kurtz & Marang (1987). It can be seen in Table 4 that the separation between the principal frequencies and their rotational sidelobes is within 1σ of the rotation frequency determined by Kurtz & Marang. This fit therefore checks whether small inaccuracies in the determination of the frequencies of the rotational sidelobes might have given rise to the secondary frequencies. It also tests for the possible presence of second-order rotational sidelobes which are expected in the oblique pulsator model for modes with $l \geq 2$.

Table 5 gives the results of a least-squares fit of ν_1 to ν_6 plus their first- and second-order rotational sidelobes to the data. Even though the least-squares fit gives an amplitude error of 0.018 mmag, there are noise peaks in the amplitude spectrum with amplitudes up to 0.08 mmag, so we rejected as noise any frequency with an amplitude less than 0.10 mmag. We also rejected $\nu_3 + 2\nu_{\rm rot}$, the only second-order rotational sidelobe with an amplitude greater than 0.10 mmag (the reason for this is that when the same fit is done and ν_{3p} plus its rotational

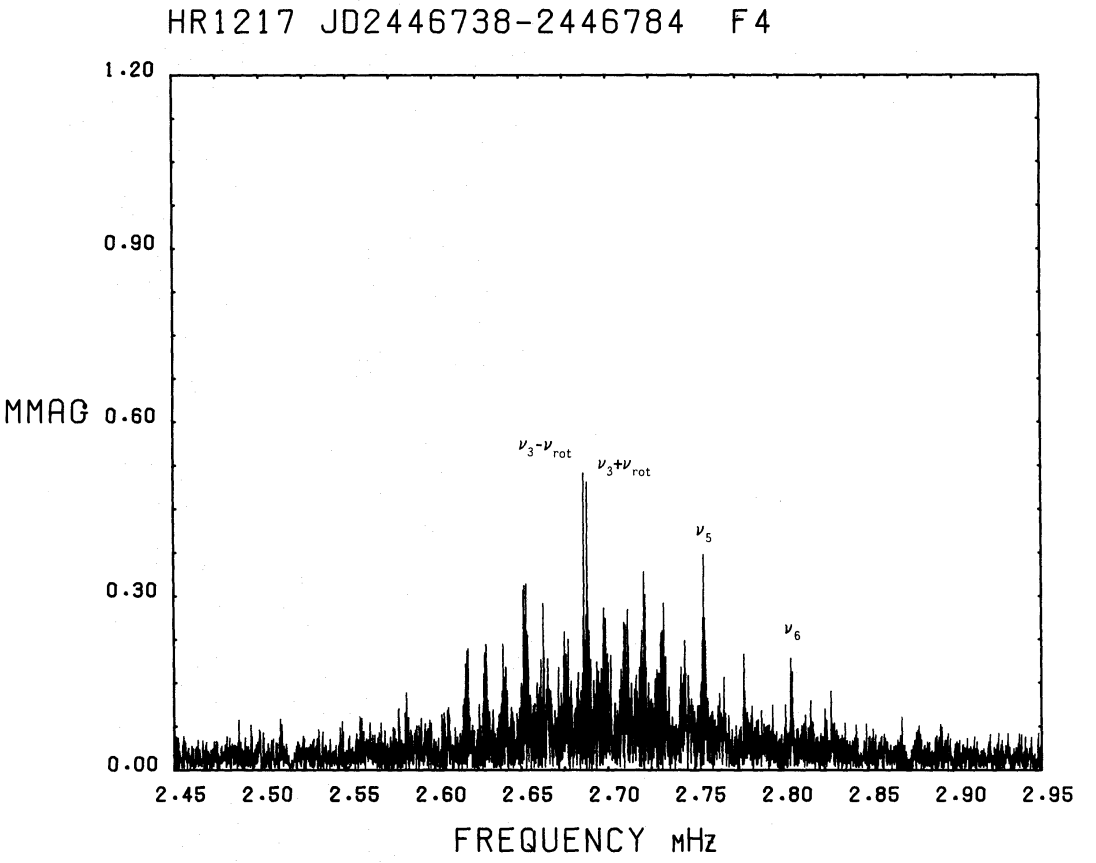

Figure 9. The amplitude spectrum of the JD2446738–2446784 *B* multi-site data after prewhitening by ν_2, ν_3 and ν_4. The highest peaks are at $\nu_3 - \nu_{rot}$ and $\nu_3 + \nu_{rot}$. The principal frequencies ν_5 and ν_6 are also labelled. The rotational sidelobes about ν_2 are easily seen also.

sidelobes are included, the amplitude of $\nu_3 + 2\nu_{rot}$ drops below 0.10 mmag; this is because ν_3 and ν_{3p} are not completely resolved) and fitted to the data by least-squares the 15 frequencies not rejected in Table 5. After prewhitening those 15 frequencies, the highest peaks in the amplitude spectrum of the residuals are at $\nu_{2p} = 2.65315$ mHz, $\nu_{4p} = 2.72112$ mHz, $\nu_{3p} = 2.68790$ mHz and $\nu_{4m} = 2.72060$ mHz – the same secondary frequencies found in the original analysis. Hence the secondary frequencies are not generated by poor identification of the rotational sidelobes.

Another reason why the secondary frequencies might be artefacts arises with the possibility that the data may not be uniform since they were collected at eight separate observatories. We show in Section 4.6 that the pulsation amplitudes are strongly a function of the wavelength of the filter used to make the observations. If the effective wavelengths of the Johnson *B* (or equivalent) filters used at the various observatories differ appreciably, then there would be amplitude differences among the various datasets which could give rise to secondary frequencies.

To check this possibility we fitted the 15 frequencies not rejected in Table 5 to the SAAO data only, which we assume are completely uniform as they were gathered with one telescope-photometer-filter combination. After prewhitening the SAAO data by the fit of those 15 frequencies, we find that the highest peak in the amplitude spectrum of the residuals is at $\nu_{4p} = 2.72114$ mHz, essentially the same as $\nu_{4p} = 2.72111$ mHz determined in the original analysis. Since that secondary frequency can be found in uniform data obtained at one site, the secondary frequencies are not artefacts generated by non-uniformity of the dataset.

Table 4. A least-squares fit of 17 derived frequencies to the JD2446738–2446784 multi-site *B* data.

name	frequency mHz ±0.00006	amp mmag ±0.018	phase radians
ν_1	2.61965	0.190	-2.07±0.09
$\nu_2-\nu_{rot}$	2.65202	0.366	-2.19±0.05
ν_2	2.65294	0.787	-2.20±0.02
$\nu_2+\nu_{rot}$	2.65395	0.202	-2.35±0.09
$\nu_3-\nu_{rot}$	2.68664	0.464	-2.38±0.04
ν_3	2.68760	1.069	-2.80±0.02
$\nu_3+\nu_{rot}$	2.68855	0.432	-2.53±0.04
ν_4	2.72085	0.863	1.07±0.02
$\nu_4+\nu_{rot}$	2.72182	0.334	1.20±0.05
ν_5	2.75569	0.288	1.81±0.06
ν_6	2.80568	0.154	1.64±0.11
$\nu_6+\nu_{rot}$	2.80661	0.147	0.40±0.12
ν_{2p}	2.65315	0.329	-2.90±0.05
ν_{3p}	2.68790	0.278	-0.21±0.07
ν_{4m}	2.72061	0.262	-0.93±0.07
ν_{4p}	2.72111	0.419	0.70±0.04
ν_{5m}	2.75515	0.210	2.38±0.09

σ=2.037 mmag

$\nu_2-(\nu_2-\nu_{rot})=\nu_{rot}$=0.92±0.08 μHz
$(\nu_2+\nu_{rot})-\nu_2=\nu_{rot}$=1.01±0.08 μHz
$\nu_3-(\nu_3-\nu_{rot})=\nu_{rot}$=0.96±0.08 μHz
$(\nu_3+\nu_{rot})-\nu_3=\nu_{rot}$=0.95±0.08 μHz
$(\nu_4+\nu_{rot})-\nu_4=\nu_{rot}$=0.97±0.08 μHz
$(\nu_6+\nu_{rot})-\nu_6=\nu_{rot}$=0.93±0.08 μHz

$\langle\nu_{rot}\rangle$=0.96±0.03 μHz
ν_{rot}(Kurtz & Marang 1987)=0.92911±0.00002 μHz

$\nu_2-\nu_1$=33.29±0.08 μHz
$\nu_3-\nu_2$=34.66±0.08 μHz
$\nu_4-\nu_3$=33.25±0.08 μHz
$\nu_5-\nu_4$=34.84±0.08 μHz
$\nu_6-\nu_5$=49.99±0.08 μHz

$\Delta_1=[(\nu_4-\nu_3)+(\nu_2-\nu_1)]/2$=33.27±0.08 μHz
$\Delta_2=[(\nu_5-\nu_4)+(\nu_3-\nu_2)]/2$=34.75±0.08 μHz

$(\nu_6-\nu_5)/\Delta_1$=1.503±0.004
$(\nu_6-\nu_5)/\Delta_2$=1.439±0.004

Note: the phase is determined from t_0 = JD2446744.15.

If we assume that the secondary frequencies are real, then the reason they are separated from the principal frequencies by about 0.25 μHz may be because that is the frequency resolution of the dataset. The principal frequencies and secondary frequencies may actually be slightly closer together or farther apart than that, but resolution problems separate them by the frequency equivalent to the length of the dataset. This supposition can potentially be tested with longer datasets. We do find that when we analyse various other subsets of the 1986 data, the exact values of the secondary frequencies are dependent on the dataset. This is possibly a resolution problem, but if the amplitude modulation of the principal frequencies is not com-

Table 5. A least-squares fit of the principal frequencies ν_1 to ν_6 and their first and second order rotational sidelobes to the JD2446738–2446784 multi-site *B* data.

Name	frequency mHz	amp mmag ±0.018	phase radians
$\nu_1-2\nu_{rot}$	2.61729	0.097	1.61±0.18 reject
$\nu_1-\nu_{rot}$	2.61872	0.091	-1.80±0.20 reject
ν_1	2.61965	0.185	-2.08±0.10
$\nu_1+\nu_{rot}$	2.62058	0.057	-1.32±0.32 reject
$\nu_1+2\nu_{rot}$	2.62151	0.046	-0.73±0.40 reject
$\nu_2-2\nu_{rot}$	2.65108	0.069	-1.91±0.27 reject
$\nu_2-\nu_{rot}$	2.65201	0.306	-2.12±0.16
ν_2	2.65294	0.789	-2.11±0.02
$\nu_2+\nu_{rot}$	2.65387	0.142	-1.56±0.13
$\nu_2+2\nu_{rot}$	2.65480	0.038	-0.22±0.49 reject
$\nu_3-2\nu_{rot}$	2.68574	0.079	-0.53±0.23 reject
$\nu_3-\nu_{rot}$	2.68667	0.415	-2.60±0.05
ν_3	2.68760	0.986	-2.81±0.02
$\nu_3+\nu_{rot}$	2.68853	0.463	-2.40±0.04
$\nu_3+2\nu_{rot}$	2.68946	0.132	-2.37±0.14 reject
$\nu_4-2\nu_{rot}$	2.71899	0.064	1.22±0.29 reject
$\nu_4-\nu_{rot}$	2.71992	0.183	1.41±0.10
ν_4	2.72085	0.854	1.10±0.02
$\nu_4+\nu_{rot}$	2.72178	0.208	1.38±0.09
$\nu_4+2\nu_{rot}$	2.72271	0.026	2.31±0.71 reject
$\nu_5-2\nu_{rot}$	2.75383	0.078	-2.30±0.24 reject
$\nu_5-\nu_{rot}$	2.75476	0.120	2.03±0.16
ν_5	2.75569	0.352	1.78±0.05
$\nu_5+\nu_{rot}$	2.75662	0.184	2.08±0.10
$\nu_5+2\nu_{rot}$	2.75755	0.060	2.06±0.31 reject
$\nu_6-2\nu_{rot}$	2.80382	0.031	-1.50±0.60 reject
$\nu_6-\nu_{rot}$	2.80475	0.048	-0.85±0.39 reject
ν_6	2.80568	0.166	1.61±0.11
$\nu_6+\nu_{rot}$	2.80661	0.157	0.34±0.12
$\nu_6+2\nu_{rot}$	2.80754	0.033	0.69±0.56 reject

σ=2.073 mmag

Note: the phase is determined from t_0 = JD2446744.15.

pletely periodic, we expect this same effect. When we fit the secondary frequencies to the data by least-squares and include their rotational sidelobes, we find that some of their rotational sidelobes have significant amplitude. This may be due to amplitude modulation of the secondary frequencies with the rotation period, or it may just be due to the amplitude modulation of the principal frequencies and the incomplete resolution of the principal frequencies and secondary frequencies.

If we assume that the oblique pulsator model applies to HR 1217, i.e. that the rotational sidelobes are separated from the principal frequencies by exactly ν_{rot}, then the 15 frequencies not rejected in Table 5 are correctly identified. After prewhitening the data by those 15 frequencies we derived a further six secondary frequencies from the amplitude spectrum of the

Table 6. A least-squares fit of derived principal frequencies, calculated rotational sidelobes, and derived secondary frequencies to the JD2446738–2446784 multi-site *B* data.

name	frequency mHz ±0.00006	amp mmag ±0.018	phase radians	$x=A_{+1}+A_{-1}/A_0$
ν_1	2.61965	0.193	-2.09±0.09	
$\nu_2-\nu_{rot}$	2.65201	0.343	-2.08±0.05	
ν_2	2.65294	0.770	-2.21±0.02	0.68±0.04
$\nu_2+\nu_{rot}$	2.65387	0.183	-1.82±0.09	
$\nu_3-\nu_{rot}$	2.68667	0.442	-2.48±0.04	
ν_3	2.68760	1.046	-2.80±0.02	0.82±0.03
$\nu_3+\nu_{rot}$	2.68853	0.418	-2.38±0.04	
$\nu_4-\nu_{rot}$	2.71992	0.156	1.28±0.11	
ν_4	2.72085	0.818	1.10±0.02	0.52±0.03
$\nu_4+\nu_{rot}$	2.72178	0.266	1.54±0.05	
$\nu_5-\nu_{rot}$	2.75476	0.170	2.15±0.10	
ν_5	2.75569	0.288	1.78±0.06	1.20±0.12
$\nu_5+\nu_{rot}$	2.75662	0.176	2.04±0.10	
ν_6	2.80568	0.160	1.61±0.11	
$\nu_6+\nu_{rot}$	2.80661	0.148	0.34±0.12	
ν_{2m}	2.65175	0.214	2.96±0.08	
ν_{2p}	2.65315	0.359	-2.96±0.05	
ν_{3p}	2.68790	0.295	-0.13±0.06	
ν_{4m}	2.72060	0.253	-0.83±0.07	
ν_{4p}	2.72112	0.449	0.59±0.04	
ν_{5m}	2.75548	0.224	2.99±0.08	

σ=2.027 mmag

Note: the phase is determined from t_0 = JD2446744.15.

residuals. A least-squares fit of those 21 frequencies is given in Table 6 and illustrated in Fig. 10.

There are important features to Tables 4 and 6 which should be noted and will be discussed in Section 5. Many of these features are the same as we found in Section 4.2 for the JD2446738–2446753 data, but are now known to higher accuracy. They are:

(i) The frequency spacing of the principal frequencies is not absolutely uniform; $\nu_2-\nu_1=\nu_4-\nu_3\equiv\Delta_1$ and $\nu_3-\nu_2=\nu_5-\nu_4\equiv\Delta_2$, where $\Delta_1<\Delta_2$. This last result is significant at the 13σ confidence level now.

(ii) The parameter $x\equiv(A_{+1}+A_{-1})/A_0$ is $x(\nu_2)=x(\nu_4)\equiv x_1$ and $x(\nu_3)\approx x(\nu_5)\equiv x_2$, where $x_1\neq x_2$.

(iii) The phases of each principal frequency and its rotational sidelobes are equal at the time of magnetic maximum. Again, as in Section 4.2, this tells us that all of the principal frequencies are at amplitude maximum at the time of magnetic maximum and are at amplitude minimum at the time of magnetic minimum.

(iv) The separation $\nu_6-\nu_5=1.503(\pm0.004)\Delta_1$.

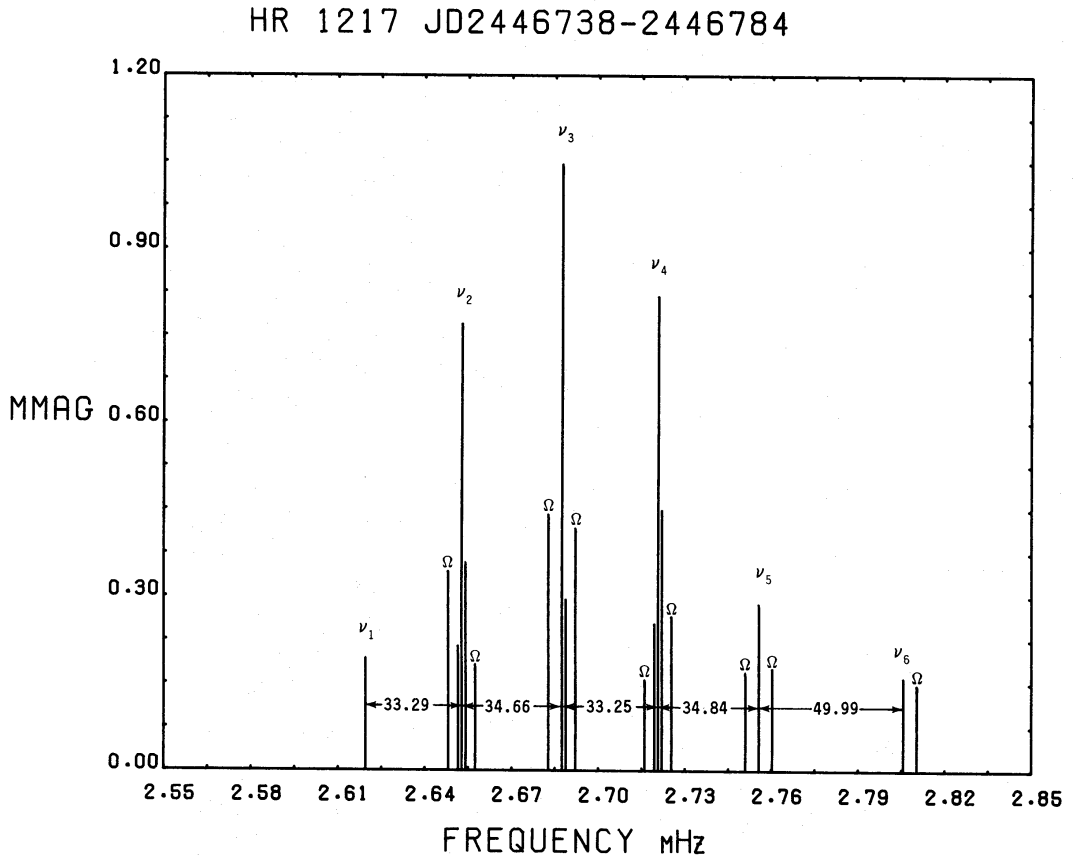

Figure 10. A schematic amplitude spectrum of the frequencies derived from the JD2446738–2446784 *B* data. A least-squares fit of these frequencies to the data is given in Table 6. The spacing of the principal frequencies is to scale; the separations are in μHz and are taken from Table 4. The rotational sidelobes are marked Ω; their separations and the separations of the secondary frequencies from the principal frequencies have been exaggerated for clarity.

(v) The secondary frequencies indicate amplitude modulation of the principal frequencies on a time-scale longer than the one rotation period studied in Section 4.2.

4.5 FREQUENCY ANALYSIS OF THE ENTIRE DATASET

We performed a frequency analysis on the entire *B* dataset listed in Table 1, but we found that the complicated window pattern led to uncertainties in the derived frequencies. This was true even for the frequencies of highest amplitude ν_2, ν_3 and ν_4. The computations were performed using the Sperry 1100/81 of the University of Cape Town, which limited us to searching 100 000 frequencies at a time. The entire dataset has a time-span of 2208 d which requires a frequency resolution of 0.2 nHz in order to have several points per peak in the amplitude spectrum. That means we were only able to search sections of the amplitude spectrum 20-μHz wide during any particular computation.

We searched the frequency space around ν_2, ν_3 and ν_4 and found $\nu_2 = 2.6529298$ mHz ($A_2 = 0.848$ mmag), $\nu_3 = 2.6876286$ mHz ($A_3 = 0.831$ mmag) and $\nu_4 = 2.7209054$ mHz ($A_4 = 0.935$ mmag). However, after simultaneously fitting ν_2 and ν_4 to the data and prewhitening, we found $\nu_3 = 2.6875322$ mHz ($A_3 = 0.730$ mmag), not the same value found before prewhitening. We did not, therefore, pursue the analysis of the entire dataset, although that would be interesting to do with much greater computing power than we had available.

An additional complication in the analysis of the entire dataset is that dv/dt, the frequency change due to the evolution of the star, may be significant over the 6-yr time-span of the data if $\nu_0 = 34\ \mu$Hz (Heller & Kawaler 1988). We cannot test for this possibility conclusively with the available data because of the confusion of the $3\,d^{-1}$ aliases in the earlier data; the window patterns of the principal frequencies are not completely resolved for those data.

4.6 THE AMPLITUDES AND PHASES AS A FUNCTION OF WAVELENGTH FROM THE MULTI-COLOUR PHOTOMETRY

As we mentioned in the introduction, both the amplitudes and phases of the principal frequencies in the rapidly oscillating Ap stars are a function of the effective wavelength of the filter through which the observations were obtained. In non-magnetic pulsating stars, such as Cepheids and δ Scuti stars, this is a result of the phase lag between the temperature and radial-velocity variations and is a function of the degree, l, of the eigenmode (Balona & Stobie 1979; Stamford & Watson 1981; Balona 1981; Watson 1988).

Several of the rapidly oscillating Ap stars have been observed through multiple filters simultaneously. HR 3831 was observed through Johnson *UBV* filters (Kurtz 1982), HD 101065 through Johnson *BV* filters (Kurtz 1980), α Cir through Johnson *BV* filters (Kurtz & Balona 1984) and through Walraven *VBLUW* filters (Weiss & Schneider 1984), and HR 1217 through Walraven *VBLUW* filters (Weiss 1986), to look at this effect, Kurtz & Balona (1984), Weiss (1986) and Watson (1988) conclude that no consistent interpretation of the amplitude ratios and phase shifts as a function of wavelength is possible for the rapidly oscillating Ap stars within the current linear theory and with current standard A star model atmospheres.

Table 7 shows a least-squares fit of the principal frequencies ν_1 to ν_6 to the ESO *uvby* data which were obtained during pulsation maximum. There appear to be no phase shifts for any of the frequencies as a function of wavelength. From the linear theory that is what we should

Table 7. A least-squares fit of the principal frequencies ν_1 and ν_6 to the ESO *uvby* data obtained from JD2446756–6760 during pulsation maximum (JD2446756.61).

	frequency mHz	A_u mmag	A_v mmag	A_b mmag	A_y mmag
ν_1	2.61965	0.51±0.11	0.80±0.09	0.48±0.09	0.36±0.09
ν_2	2.65294	0.72±0.12	1.25±0.10	0.58±0.10	0.42±0.10
ν_3	2.68760	1.36±0.12	1.92±0.10	1.06±0.10	0.65±0.10
ν_4	2.72085	0.76±0.13	1.21±0.10	0.58±0.10	0.27±0.10
ν_5	2.75569	0.66±0.13	0.87±0.10	0.55±0.10	0.33±0.10
ν_6	2.80568	0.43±0.11	0.76±0.09	0.36±0.10	0.23±0.09
	frequency mHz	ϕ_u radian	ϕ_v radian	ϕ_b radian	ϕ_y radian
ν_1	2.61965	-2.42±0.22	-2.43±0.11	-2.22±0.19	-2.23±0.25
ν_2	2.65294	-1.34±0.17	-1.35±0.08	-1.14±0.17	-1.39±0.24
ν_3	2.68760	-3.05±0.09	-2.94±0.05	-2.81±0.09	-2.82±0.15
ν_4	2.72085	2.40±0.17	2.58±0.08	2.76±0.17	2.73±0.31
ν_5	2.75569	1.97±0.20	2.13±0.12	2.09±0.19	2.30±0.31
ν_6	2.80568	1.71±0.27	2.05±0.12	2.34±0.25	2.21±0.39

Note: the phases are calculated with respect to t_0 = JD2446744.15.

expect for l = odd modes; at face-value this would seem to support the interpretation that the principal frequencies are due to l = odd eigenmodes of consecutive n and that $\nu_0 = 34\ \mu$Hz. However, since the linear theory does not give consistent interpretations of the phase shifts seen in HR 3831, HD 101065 and α Cir (Kurtz & Balona 1984; Weiss 1986; Watson 1988), we do not think that the results of Table 7 rule out other mode identifications for the principal frequencies.

Table 7 shows that the frequencies all have their highest amplitudes in the Strömgren v filter ($\lambda_{\rm eff} = 4100$ Å); of the Strömgren filters, this is the one closest to the Johnson B filter ($\lambda_{\rm eff} = 4350$ Å). The amplitudes in Strömgren y are only about 1/3 those in Strömgren v. Table 8 shows a least-squares fit of the principal frequencies to the Lowell Observatory BV data which were also obtained during pulsation maximum. Again, there is no evidence of phase shifts for any of the frequencies. The V amplitudes are less than half of the B amplitudes.

Table 8. A least-squares fit of the principal frequencies ν_1 and ν_6 to the LO BV data obtained from JD2446743–6747 during pulsation maximum (JD2446744.15).

	frequency mHz	A_B mmag	A_V mmag	ϕ_B radian	ϕ_V radian
ν_1	2.61965	0.49±0.08	0.11±0.07	-1.82±0.15	-0.90±0.65
ν_2	2.65294	1.66±0.10	0.68±0.09	-2.14±0.06	-2.10±0.13
ν_3	2.68760	0.96±0.10	0.31±0.09	3.04±0.10	-3.08±0.29
ν_4	2.72085	1.00±0.10	0.44±0.09	0.76±0.10	0.96±0.21
ν_5	2.75569	0.46±0.10	0.05±0.09	2.07±0.21	-3.04±2.07
ν_6	2.80568	0.06±0.08	0.29±0.07	2.25±1.25	2.27±0.25

Note: the phases are calculated with respect to t_0 = JD2446744.15.

5 Discussion

We assume throughout this discussion that HR 1217 is an oblique pulsator. Several lines of evidence support this assumption:

(i) The rotational sidelobes found in the frequency analyses of the JD2446738–2446753 data (Section 4.2) and the JD2446738–2446784 data (Section 4.4) are split from their principal frequencies precisely by the rotation frequency, to an accuracy of ± 30 nHz in the latter case. This argues either for oblique pulsation or the excitation of rotationally perturbed m-modes.

(ii) As we pointed out in the introduction, the data now available show that if m-modes are excited, $C_{n,l} \leq 0.0006$ at the 3σ confidence level (see equaiton 2). This is much less than the expected value of $C_{n,l} \approx 0.01$ (Shibahashi & Saio 1985). In addition, the observed coincidence of pulsation maximum and magnetic maximum is purely accidental if the rotational sidelobes are due to excited m-modes, whereas it is required by the oblique pulsator model.

(iii) The amplitude modulation of the pulsational radial velocity variations found by Matthews *et al.* (1988) favours the oblique pulsator model over the spotted pulsator model (Mathys 1985).

We note here that the principal frequencies are secure, since they can be derived from independent datasets. Table 9 compares the values found for the principal frequencies in Sections 4.4, 4.2 and 4.1 with those found by Kurtz & Seeman (1983) 5 yr earlier. All are the same except for Kurtz & Seeman's ν_6 which differs by 0.012 mHz = 1 d^{-1}; for that frequency it appears that Kurtz & Seeman were confused by a 1 d^{-1} alias. In their analysis ν_6 did not stand out well above the noise and they were uncertain about its reality.

Table 9. A comparison between the frequencies derived by Kurtz & Seeman (1983) and the principal frequencies found in this paper.

	(1) mHz ±0.00006	(2) mHz ±0.0002	(3) mHz ±0.004	(4) mHz ±0.002
ν_1	2.61965	2.6195	2.627	2.620
ν_2	2.65294	2.6530	2.654	2.653
ν_3	2.68760	2.6875	2.684	2.688
ν_4	2.72085	2.7210	2.725	2.721
ν_5	2.75569	2.7554	2.751	2.756
ν_6	2.80568	2.8062	2.803	2.794

(1) This paper, JD2446738-2446784 data; Section 4.4.
(2) This paper, JD2446738-2446753 data; Section 4.2.
(3) This paper, 15.73-hr data at amplitude maximum (Fig. 2); Section 4.1.
(4) Kurtz & Seeman (1983)

5.1 THE MAGNETIC FIELD, ROTATIONAL INCLINATION, AND MAGNETIC OBLIQUITY

Following Kurtz & Marang (1987) we have fitted the function

$$B_e = B_0 + B_1\cos[2\pi\nu_{rot}(t-t_0)+\phi_1] + B_2\cos[4\pi\nu_{rot}(t-t_0)+\phi_2] \quad (4)$$

by least-squares to the magnetic observations of Preston (1972) and Landstreet (1983, private communication). We find that the coefficient B_2 is not significantly different from zero indicating that the magnetic observations are adequately described by a simple sinusoid; we therefore assume that the magnetic variations of HR 1217 are due to a centred dipole oblique rotator. Our time of magnetic maximum, $t_0 = \text{JD}2440577.2 \pm 0.2$, is the same as that given by Kurtz & Marang and is, therefore, the same as the time of pulsation maximum, within the errors (see Section 3). From our least-squares fit we find $B_0 = 865 \pm 31$ G and $B_1 = 452 \pm 43$ G. For an oblique rotator, magnetic variations are often characterized by the parameter $r \equiv B_e(\text{min})/B_e(\text{max})$, where $-1 \le r \le +1$; in this case $B_e(\text{min}) = B_0 - B_1$ and $B_e(\text{max}) = B_0 + B_1$ which yields $r = 0.31 \pm 0.04$. It is easy to show for an oblique rotator that

$$\tan i \tan\beta = (1-r)/(1+r), \quad (5)$$

where i is the rotational inclination and β is the magnetic obliquity. Equation (5) gives $\tan i \tan\beta = 0.52 \pm 0.03$ for HR 1217.

Table 10 gives the allowed values of i and β under the constraint that $\tan i \tan\beta = 0.52$. It also lists the values of $\alpha_{min} = \beta - i$, the minimum angle between the magnetic pole and the line of sight and the angle at which a dipole field will show maximum effective field strength. The polar field strength, B_p, is then $B_p = B_e(\text{max})/(0.310\cos\alpha_{min})$, calculated under the assumption of a limb-darkening law of the form

$$I(\theta) = 1 - k + k\cos\theta$$

and $k = 0.5$ (Schwarzschild 1950). The factor in the denominator (0.310 for a dipole) is easily derived from a normalized integration of $P_{l+1}(\cos\theta)$ seen pole-on and weighted by the limb-darkening. The appropriate Legendre polynomial is $P_{l+1}(\cos\theta)$, rather than $P_l(\cos\theta)$, because it is only the longitudinal component of the magnetic field which produces a measurable Zeeman effect for the techniques normally used for Ap star magnetic observations.

For the smallest rotational inclination which we list in Table 10, $i = 1°.0$, we find that $B_p \approx 82\,000$ G. If we require that HR 1217 have a polar field strength no greater than the

Table 10. The allowed values of i and β given $\tan i \tan \beta = 0.52$ from the magnetic field measurements, the minimum and maximum angles between the magnetic (pulsation) pole and the line-of-sight, and the relative amplitudes of the central frequency component of the $(2l+1)$-multiplet for $l = 1, 2$ and 3, $m = 0$.

i	β	α_{min}	α_{max}	$A_0^{(1)}/\varepsilon_{n,1}$	$A_0^{(2)}/\varepsilon_{n,2}$	$A_0^{(3)}/\varepsilon_{n,3}$	y
1.0	88.1	87.1	89.1	0.024	-0.164	-0.003	-0.003
2.0	86.1	84.1	88.1	0.048	-0.162	-0.006	-0.014
3.0	84.2	81.2	87.2	0.072	-0.159	-0.009	-0.033
4.0	82.3	78.3	86.3	0.095	-0.155	-0.012	-0.059
5.0	80.4	75.4	85.4	0.118	-0.150	-0.014	-0.095
6.0	78.6	72.6	84.6	0.140	-0.143	-0.016	-0.139
7.0	76.7	69.7	83.7	0.162	-0.136	-0.018	-0.198
8.0	74.9	66.9	82.9	0.183	-0.128	-0.020	-0.269
9.0	73.1	64.1	82.1	0.204	-0.119	-0.021	-0.359
10.0	71.3	61.3	81.3	0.224	-0.109	-0.022	-0.472
15.0	62.7	47.7	77.7	0.315	-0.055	-0.022	-1.842
20.0	55.0	35.0	75.0	0.383	-0.002	-0.016	-84.331
25.0	48.1	23.1	73.1	0.430	0.041	-0.008	4.617
30.0	42.0	12.0	72.0	0.457	0.068	-0.002	3.147
35.8	35.8	0.0	71.6	0.467	0.078	0.001	2.850

Note: for values of $i > 35.8°$ or $\beta < 35.8°$, reverse the column headings.

largest known, $B_p \approx 213\,000$ G in HD 215441 (Borra & Landstreet 1980), then the only restriction we can put on i based on the field strength is $i > 0.^{\circ}4$.

Matthews *et al.* (1988) obtained digital spectra of HR 1217 with the Canada–France–Hawaii 3.6-m telescope (CFHT) using integration times which were 0.1 of the pulsation period for $\nu_4 = 2.720$ mHz (36.76 s). Spectra from the same pulsation phase were then binned with a resultant signal-to-noise ratio of about 150, and from these spectra they discovered 400 m s^{-1} radial velocity variations.

From those same spectra we estimate the rotational velocity of HR 1217 to be $v \sin i \leq 1.0$ km s^{-1}. However, Bohlender (private communication) has modelled several spectral lines for similar spectra obtained by Landstreet with the CFHT, and he estimates $v \sin i \approx 5$ km s^{-1}. We have not yet resolved this discrepancy; we can only state with confidence that $v \sin i \leq 7$ km s^{-1} for HR 1217.

This puts very little constraint on i. Given the 12.4572-d rotation period of HR 1217, and using the models of Heller & Kawaler (1988), we find $R = 2.3\,R_\odot$ if $\nu_0 = 68\,\mu$Hz ($v_{rot} = 9.4$ km s^{-1} and $i \leq 48°$) and $R = 3.2\,R_\odot$ if $\nu_0 = 34\,\mu$Hz ($v_{rot} = 13.1$ km s^{-1} and $i \leq 32°$). Referring to Table 10, we see that for $i \leq 48°$, $\beta \geq 25°$ and for $i \leq 32°$, $\beta \geq 40°$. It appears that the rotation axis of HR 1217 is not inclined very far from the line-of-sight and it may be nearly pole-on. A stronger constraint than this will have to await a high-accuracy measurement of $v \sin i$.

5.2 CONSTRAINTS ON THE PULSATION MODELS

The amplitude modulation of an oblique dipole pulsation mode has the same dependence on i, β and the rotation frequency as does the magnetic variation of an oblique dipole rotator; both are modulated as

$$\cos \alpha = \cos i \cos \beta + \sin i \sin \beta \cos \Omega t, \tag{6}$$

where α is the angle between the pulsation (magnetic) pole and the line-of-sight, Ω is the rotational frequency, and phase is measured from amplitude (magnetic) maximum. This means

that any of the principal frequencies which are dipole modes should have the same value of $\tan i \tan \beta = 0.52 \pm 0.03$ as does the magnetic field.

For a dipole oblique pulsation $x \equiv (A^{(1)}_{+1} + A^{(1)}_{-1})/A^{(1)}_0 = \tan i \tan \beta$ (Shibahashi 1986; Kurtz & Shibahashi 1986). From Tables 6 and 3 we can see that ν_2 and ν_4 have the same $\tan i \tan \beta$ as the magnetic field. That suggests that ν_2 and ν_4 are dipole eigenmodes. The fact that $x(\nu_3)$ and $x(\nu_5)$ are *not* the same as $\tan i \tan \beta$ for the magnetic field suggests that they are *not* due to dipole eigenmodes.

Dziembowski (1977) calculates the integrated bolometric luminosity variations for a non-radially oscillating star, taking into account both flux and radius variations and assuming an Eddington limb-darkening law. The flux variations include a scale factor f which Balona & Stobie (1979) find is typically on the order of $f = 10$ for δ Scuti stars and Cepheids. From arguments based on the radial velocity variations, Kurtz (1982) estimated that $f > 10$ for the rapidly oscillating Ap stars.

For $f > 10$, the relative observed amplitudes in an oblique pulsator are approximately

$$\Delta M_{\rm bol} \propto \varepsilon_{n,l} b_l P_l(\cos \alpha), \tag{7}$$

where $\varepsilon_{n,l}$ is a factor linearly proportional to the excitation amplitude, b_l results from the normalized integration of the spherical harmonic over the visible surface weighted by the limb-darkening, and $\cos \alpha$ is given by equation (6).

In an oblique pulsator each normal mode gives rise to $(2l+1)$ observed frequencies; we refer to the amplitude of the central frequency as $A^{(l)}_0$ (Shibahashi 1986; Kurtz & Shibahashi 1986). For $l = 0, 1, 2, 3$ $(m = 0)$ modes we then have

$$A^{(0)}_0 = \varepsilon_{n,0} \tag{8}$$

$$A^{(1)}_0 = 0.71 \varepsilon_{n,1} \cos i \cos \beta \tag{9}$$

$$A^{(2)}_0 = 0.33 \varepsilon_{n,2} \tfrac{1}{24} (3 \cos^2 \beta - 1)(3 \cos^2 i - 1) \tag{10}$$

$$A^{(3)}_0 = 0.06 \varepsilon_{n,3} \tfrac{1}{64} (3 \cos \beta + 5 \cos 3\beta)(3 \cos i + 5 \cos 3i). \tag{11}$$

In Table 10 the values of A_0 for $l = 1, 2$ and 3 are listed for the allowed values of i and β assuming that $\varepsilon_{n,l}$ is the same for each mode. For $i \geq 1°$, we can see that an $l = 3$ mode would have to have an intrinsic amplitude at least 8 times greater than that of an $l = 1$ mode to have an equivalent A_0. This makes modes with $l = 3$ unlikely to be observed, and modes with higher l even less likely.

From Kurtz & Shibahashi (1986) we have for a quadrupole mode

$$A^{(2)}_{+1} + A^{(2)}_{-1}/A^{(2)}_0 = 12 \sin \beta \cos \beta \sin i \cos i / (3 \cos^2 \beta - 1)(3 \cos^2 i - 1) \equiv y, \tag{12}$$

where we have listed the values of y in Table 10 given i and β. The negative values of y indicate that the central frequency of the frequency triplet for a quadrupole mode is 180° out of phase with the outside pair of frequencies. It is easy to see from Table 6 that the phases are the same for the frequency triplets, ruling out $l = 2$, $m = 0$ for all i, β pairs for which $y < 0$ which includes all $i \leq 20°$.

We can rule out other values of i, β, too. Between $i = 20°$ and $i = 25°$ the value of y goes to $-\infty$ and returns from $+\infty$. This simply reflects the central frequency of the frequency triplet going from negative amplitude to positive amplitude through zero. For i, β pairs where y is positive, $y \geq 2.85$. If any of the principal frequencies are due to quadrupole modes, then $y = x = (A_{+1} + A_{-1})/A_0$ and Table 6 shows the measured values of $x \leq 1.20$. There is no way to accommodate values of $y \geq 2.85$ even though the true errors on x are probably greater than the

internal errors quoted (because the frequency analysis is not complete). Thus we can rule out $l=2$, $m=0$ for the principal frequencies ν_2, ν_3, ν_4 and ν_5 for all allowed i and β.

We have already argued that $l=3$ modes are unlikely due to their low apparent amplitude (unless they are excited to much higher intrinsic amplitude then the dipole modes). Radial modes are ruled out by the presence of the rotational sidelobes; the amplitude of an $l=0$ mode is not dependent on aspect. We can also rule out modes with $l=1$ or 2 and $m\neq 0$.

In the simplest form of the oblique pulsator model, where the effects of the magnetic field and Coriolis forces are neglected, the observable luminosity variation can be written as

$$\Delta L/L \propto Y_{lm}(\cos\alpha)\cos(\omega t+\phi), \tag{13}$$

where $\cos\alpha$ is given by equation (6). The modes $l=1$, $m=\pm 1$ and $l=2$, $m=\pm 2$ are ruled out because $P_{11}(\cos\alpha)\propto\sin\alpha$ and $P_{22}(\cos\alpha)\propto\sin^2\alpha$, both of which have larger amplitudes at magnetic minimum than at magnetic maximum.

The case for $l=2$, $m=\pm 1$ modes is more complicated, since $P_{21}\propto\cos\alpha\sin\alpha$, which has a larger amplitude at magnetic maximum than at magnetic minimum for HR 1217. Again we simplify the oblique pulsator model by ignoring the magnetic and Coriolis effects. This then yields a simple expression for the observed luminosity variation (Shibahashi 1986; Kurtz & Shibahashi 1986) of

$$\Delta L/L \propto \sum_{m'=-l}^{+l}(-1)^{m'}\mathbf{d}^{(l)}_{mm'}(\beta)\mathbf{d}^{(l)}_{m'0}(i)\cos[(\omega_0-m'\Omega)t+\phi], \tag{14}$$

where the matrix $\mathbf{d}^{(2)}_{m'm}(\beta)$ is given in Table 11 [for $\mathbf{d}^{(1)}_{m'm}(\beta)$ see Kurtz & Shibahashi 1986]. We find from this that the A_{+1} and A_{-1} components for $l=2$, $m=\pm 1$ are in antiphase with each other at the time of magnetic maximum for the values of i and β given in Table 10. This is in conflict with the observations, and hence these modes are also ruled out for HR 1217. More complex calculations including the effects of the magnetic field and Coriolis force do not change these results.

This leaves us with only dipole modes to explain ν_2, ν_3, ν_4 and ν_5. As we have said before, the ratio $x=(A_{+1}+A_{-1})/A_0$ for ν_2 and ν_4 is consistent with $\tan i\tan\beta$ from the magnetic measurements, but the same is not true for ν_3 and ν_5. We therefore conclude that ν_3 and ν_5 cannot be explained by purely normal modes. The larger values of $x(\nu_3)=0.82\pm 0.03$ and $x(\nu_5)=1.20\pm 0.12$ indicate that these modes have amplitude minima smaller than would be expected for dipole modes; their amplitudes go more nearly to zero at magnetic minimum than does the amplitude of a dipole mode.

Table 11. The matrix $\mathbf{d}^{(2)}_{m'm}(\beta)$.

$\frac{1}{4}(1+\cos\beta)^2$	$\frac{1}{2}\sin\beta(1+\cos\beta)$	$\frac{\sqrt{3}}{2\sqrt{2}}\sin^2\beta$	$\frac{1}{2}\sin\beta(1-\cos\beta)$	$\frac{1}{4}(1-\cos\beta)^2$
$-\frac{1}{2}\sin\beta(1+\cos\beta)$	$\frac{1}{2}(2\cos\beta-1)(1+\cos\beta)$	$\frac{\sqrt{3}}{\sqrt{2}}\sin\beta\cos\beta$	$\frac{1}{2}(2\cos\beta-1)(1-\cos\beta)$	$\frac{1}{2}\sin\beta(1-\cos\beta)$
$\frac{\sqrt{3}}{2\sqrt{2}}\sin^2\beta$	$-\frac{\sqrt{3}}{\sqrt{2}}\sin\beta\cos\beta$	$\frac{1}{2}(3\cos^2\beta-1)$	$\frac{\sqrt{3}}{\sqrt{2}}\sin\beta\cos\beta$	$\frac{\sqrt{3}}{2\sqrt{2}}\sin^2\beta$
$-\frac{1}{2}\sin\beta(1-\cos\beta)$	$\frac{1}{2}(2\cos\beta+1)(1-\cos\beta)$	$-\frac{\sqrt{3}}{\sqrt{2}}\sin\beta\cos\beta$	$\frac{1}{2}(2\cos\beta-1)(1+\cos\beta)$	$\frac{1}{2}\sin\beta(1+\cos\beta)$
$\frac{1}{4}(1-\cos\beta)^2$	$-\frac{1}{2}\sin\beta(1-\cos\beta)$	$\frac{\sqrt{3}}{2\sqrt{2}}\sin^2\beta$	$-\frac{1}{2}\sin\beta(1+\cos\beta)$	$\frac{1}{4}(1+\cos\beta)^2$

Note: the rows correspond to $m'=2, 1, 0, -1, -2$ from top-to-bottom and the columns correspond to $m=2, 1, 0, -1, -2$ from left-to-right.

To summarize this section: The principal frequencies ν_2, ν_3, ν_4 and ν_5 each have first rotational sidelobes which are in phase with them at the time of magnetic maximum. We rule out $l=0$ modes based on the presence of the rotational sidelobes; we rule out $l=2$, $m=0$ modes based on the phasing of the rotational sidelobes; we regard $l\geq 3$ modes as improbable based on the lower integrated observed amplitude for higher degree modes; we rule out $l=1$, $m=\pm 1$ modes and $l=2$, $m=\pm 1, \pm 2$ modes based also on the phases of the rotational sidelobes. The only eigenmode with $l\leq 2$ which has pulsation maximum at the time of magnetic maximum and also has the principal frequency and rotational sidelobes in phase at the time of magnetic maximum is the $l=1$, $m=0$ mode. The amplitudes of the rotational sidelobes of ν_2 and ν_4 are consistent with the expected values for an oblique dipole pulsator; those of ν_2 and ν_4 are consistent with the expected values for an oblique dipole pulsator; those of ν_3 and ν_5 are not. We conclude that ν_2 and ν_4 are $l=1$, $m=0$ modes and the ν_3 and ν_5 are not normal modes.

5.3 THE FREQUENCY SPACINGS

The spacing of the principal frequencies given in Table 6 and illustrated in Fig. 10 is what led Shibahashi (1984) to suggest that they are due to alternating even and odd l-modes. Shibahashi and Saio (1985) suggested that the inequality $\Delta_1 < \Delta_2$ favoured $l=0$ modes over $l=2$ modes for ν_3 and ν_5. We have shown in the last section that ν_3 and ν_5 cannot be due to either $l=0$ or 2; they must be due to non-normal modes.

In the last section we showed that ν_3 and ν_5 look similar to dipole modes, but that they have amplitude minima smaller than expected. If we assume that ν_1, ν_2, ν_3, ν_4 and ν_5 are due to dipole modes of consecutive overtone, n, and that some additional factor modifies the amplitudes of ν_3 and ν_5, then $\nu_0 = 34\,\mu$Hz (Heller & Kawaler 1988) and the radius of HR 1217 is $R=3.2\,R_\odot$; that leads to the constraint $i\leq 32°$ (Section 5.1). The problem with this interpretation is that it does not simply explain the alternating Δ_1, Δ_2 frequency spacing. From equation (1) we would expect naïvely that the frequency spacing between consecutive overtones of the same l should be constant.

The alternating Δ_1, Δ_2 spacing of ν_1, ν_2, ν_3, ν_4 and ν_5 is more suggestive of alternating even and odd $l=$ modes with $\nu_0 = 68\,\mu$Hz. This yields $R=2.3\,R_\odot$ and $i\leq 48°$. For this interpretation to be correct, ν_1, ν_3 and ν_5 need to be excited radial ($l=0$) modes which have been modified to have the observed amplitude modulation. We cannot say whether that is more or less likely than modified $l=1$ modes, which is the other interpretation.

The separation $\nu_6 - \nu_5 = 1.503\Delta_1$ can be interpreted with equation (1) if $\nu_0 = 34\,\mu$Hz. Then ν_1, ν_2, ν_3, ν_4 and ν_5 are all $l=1$ modes of overtone n, $n+1$, $n+2$, $n+3$ and $n+4$, respectively, and ν_6 is an $n+5$, $l=2$ mode. We can think of no reasons why that particular $l=2$ mode should be excited and no others. That ν_6 appears to be a frequency doublet with components which are in phase a quarter of a cycle after magnetic maximum (Table 6) suggests that ν_6 is not due to a dipole mode. The amplitudes of the two components of ν_6 are close enough to our noise level, however, that we cannot rule out the possibility that a third component is present, but masked by the noise. On the other hand, if we accept the $\nu_0 = 68\,\mu$Hz interpretation of alternating even and odd l-modes, then there is no way at all to interpret ν_6 in terms of equation (1).

5.4 THE SECONDARY FREQUENCIES

The secondary frequencies listed in Tables 4 and 6 indicate that the principal frequencies are amplitude modulated on a time-scale of weeks to months (or possibly longer). They are

unlikely to be due to eigenmodes of $(n-1, l+2)$ or $(n+1, l-2)$ (see equation 1); such modes are expected from model calculations to be separated from the principal frequencies by about 3–6 μHz (Shibahashi & Saio 1985), and there is no straightforward way to explain frequencies both higher and lower than the principal frequency, such as ν_{4p} and ν_{4m}, where ν_4 is due to a dipole mode.

The secondary frequencies indicate that the amplitudes of the principal frequencies grow and decay on a time-scale of weeks to months. That could be caused by mode coupling or by low-level fluctuations in the driving process, which is unknown (Shibahashi 1987). Another rapidly oscillating Ap star, HD 60435, appears to pulsate in modes with amplitudes which are variable on a time-scale of weeks (Matthews, Kurtz & Wehlan 1986, 1987). It may be significant that HD 60435 has many frequencies separated by $\sim 26\,\mu$Hz. Another rapidly oscillating Ap star, HR 3831 (Kurtz & Shibahashi 1986), appears to be stable in amplitude over a time-scale of years, but it has only one principal frequency.

5.5 THE INEQUALITY OF THE A_{+1} AND A_{-1} COMPONENTS

In the oblique pulsator model the relative amplitudes of the rotational sidelobes of a dipole mode are dependent on the ratio of the effect of the Coriolis force to the magnetic perturbation. In particular

$$(A^{(1)}_{+1} - A^{(1)}_{-1})/(A^{(1)}_{+1} + A^{(1)}_{-1}) = C_{n,l}\Omega/(\omega^{(1)\,\mathrm{mag}}_{1} - \omega^{(1)\,\mathrm{mag}}_{0}) \equiv z \qquad (15)$$

(Kurtz & Shibahashi 1986), where $C_{n,l}$ is the rotational splitting constant from equation (2), Ω is the rotation frequency, and the $\omega^{(1)\,\mathrm{mag}}_{|m|}$ are the perturbations to the pulsation frequency due to the magnetic field. For HR 3831 Kurtz & Shibahashi (1986) find $z = -0.10$ and for HD 6532 Kurtz & Cropper (1987) find $z = -0.24$. In both cases the value of z indicates that the magnetic perturbation dominates over the Coriolis force.

The pulsation frequency perturbation, $\omega^{(1)\,\mathrm{mag}}_{|m|}$, is dependent on a $|Y_{lm}|^2$-weighted integration over the distortion by the magnetic field, and hence is a measure of the magnetic field throughout the star. Unfortunately, for HR 1217 the values of z are not consistent for the principal frequencies. We have argued above that ν_2 and ν_4 are due to dipole modes. In that case, from the data in Table 6 $z(\nu_2) = -0.30 \pm 0.05$ and $z(\nu_4) = +0.26 \pm 0.06$. Because of the opposite signs, these two are completely inconsistent with each other. We do not know whether this is due to unresolved frequencies altering the values for A_{+1} and A_{-1}, whether either one or both ν_2 and ν_4 are not dipole modes, or whether the model applied is not correct. In the two cases of HR 3831 and HD 6532, only a single frequency triplet is used in each star to calculate z, and hence there is no check for inconsistency as there is in the case of HR 1217. The value of $z(\nu_2) = -0.30$ is essentially the same as that found for HD 6532; had ν_2 been the only pulsation frequency present, we would have concluded that the magnetic fields of HR 1217 and HD 6532 must be similar. The positive value of $z(\nu_4)$ indicates that that would be a premature conclusion.

We also note here that $z(\nu_3) = 0.00 \pm 0.03$ and $z(\nu_5) = 0.02 \pm 0.07$. The meaning of those values is not clear since ν_3 and ν_5 are not due to normal modes.

5.6 THE CRITICAL FREQUENCY

The critical frequency depends on the wavelength of the oscillation compared to the pressure scale-height. When the linear distance over which a standing wave is reflected at the stellar surface is long compared with the wavelength of the oscillation, then phase coherence is lost and the standing wave cannot be maintained. Shibahashi & Saio (1985) calculate that the

critical frequency for normal A star models is lower than the frequencies observed in HR 1217. This problem needs to be studied including the effects of the magnetic field which should increase the critical frequency since the magnetic field provides additional resistance to acoustic waves in ionized gases.

5.7 CONCLUSIONS

From the analyses presented in this paper and from the discussion above, we come to the following conclusions.

(i) HR 1217 is an oblique rotator with a centred dipole magnetic field. The geometry of the field requires that $\tan i \tan \beta = 0.52 \pm 0.03$.

(ii) HR 1217 is an oblique pulsator with the pulsation axis and the magnetic axis aligned. This is required by the coincidence of the times of amplitude maximum and magnetic maximum.

(iii) There are six principal frequencies of pulsation in HR 1217. We find that ν_2 and ν_4 are dipole modes ($l=1$, $m=0$); ν_3 and ν_5 cannot be due to normal modes – they look similar to dipole modes, but they have amplitude minima which are lower than expected.

(iv) It is not possible to discriminate between the hypothesis that ν_1, ν_2, ν_3, ν_4 and ν_5 are basically due to alternating even and odd l-modes with $\nu_0 = 68\ \mu$Hz, and the hypothesis that they are all basically due to dipole modes with $\nu_0 = 34\ \mu$Hz. The sixth principal frequency, ν_6, could be an $l=2$ mode if $\nu_0 = 34\ \mu$Hz, but then the alternating Δ_1, Δ_2 frequency spacing is inexplicable. If $\nu_0 = 68\ \mu$Hz, then the Δ_1, Δ_2 spacing makes sense but the $\nu_6 - \nu_5 = 1.503\,\Delta_1$ spacing is inexplicable.

(v) The secondary frequencies indicate that the principal frequencies are amplitude modulated on a time-scale of months. This is not likely to be due to pulsation in higher degree modes, and hence indicates that the amplitudes of the principal frequencies are not completely stable.

Acknowledgments

DWK thanks the director of SAAO, Professor M. W. Feast, for providing five weeks of continuous observing time on the SAAO 1.0-m telescope around which this project was organized. He also thanks the computing centre of the University of Cape Town for the generous allotment of computing time necessary for the analysis of the data presented in this paper. He acknowledges support from the Foundation for Research Development of the CSIR. JMM thanks the director and staff of the Institute for Astronomy's Mauna Kea Observatory for the generous allocation of observing time and technical support. His participation was partially funded by a grant to W. H. Wehlau from the Natural Sciences and Engineering Research Council of Canada. MC acknowledge support by a SERC AAT Fellowship and thanks the director of MSSSO for the allocation of telescope time. TJK thanks the Lowell Observatory for providing support for this project. CS acknowledges a research grant from NFWO–Belgium. SDK acknowledges support from NASA grant NAGP-778. WWW acknowledges support by the Austrian Fonds zur Förderung der wissenshaftlichen Forschung, project No. 4170. AvdP and DJS thank Canterbury University for the allocation of Mt John telescope time and they acknowledge financial support from both the research fund of the NZ University Grants Committee and the VUW Internal Research Committee. We thank Dr John Landstreet for kindly providing his unpublished magnetic data, and Dr Dave Bohlender for modelling his spectra of HR 1217 to provide us with an estimate of $v \sin i$.

References

Balona, L. A., 1981. *Mon. Not. R. astr. Soc.*, **196,** 159.
Balona, L. A. & Stobie, R. S., 1979. *Mon. Not. R. astr. Soc.*, **189,** 649.
Bonsack, W. K., 1979. *Publs astr. Soc. Pacif.*, **91,** 648.
Borra, E. F. & Landstreet, J. D., 1980. *Astrophys. J. Suppl.*, **42,** 421.
Breger, M., 1988. *Publs astr. Soc. Pacif.*, **100,** 751.
Deeming, T. J., 1975. *Astrophys. Space Sci.*, **36,** 137.
Dziembowski, W., 1977. *Acta astr.*, **27,** 203.
Dziembowski, W. & Goode, P. R., 1985. *Astrophys. J.*, **296,** L27.
Dziembowski, W. & Goode, P. R., 1986. In: *Seismology of the Sun and Distant Stars,* p. 441, ed. Gough, D. O., Reidel, Dordrecht.
Gabriel, M., Noels, A., Scuflaire, R. & Mathys, G., 1985. *Astr. Astrophys.*, **143,** 206.
Heller, C. H. & Kawaler, S. D., 1988. *Astrophys. J.*, **329,** L43.
Kurtz, D. W., 1980. *Mon. Not. R. astr. Soc.*, **191,** 115.
Kurtz, D. W., 1982. *Mon. Not. R. astr. Soc.*, **200,** 807.
Kurtz, D. W., 1985. *Mon. Not. R. astr. Soc.*, **213,** 773.
Kurtz, D. W., 1986. In: *Seismology of the Sun and Distant Stars,* p. 417, ed. Gough, D. O., Reidel, Dordrecht.
Kurtz, D. W., 1988. *Mon. Not. R. astr. Soc.*, **233,** 565.
Kurtz, D. W. & Balona, L. A., 1984. *Mon. Not. R. astr. Soc.*, **210,** 779.
Kurtz, D. W. & Seeman, J., 1983. *Mon. Not. R. astr. soc.*, **205,** 11.
Kurtz, D. W. & Shibahashi, H., 1986. *Mon. Not. R. astr. Soc.*, **223,** 557.
Kurtz, D. W. & Cropper, M. S., 1987. *Mon. Not. R. astr. Soc.*, **228,** 125.
Kurtz, D. W. & Marang, F., 1987. *Mon. Not. R. astr. Soc.*, **229,** 285.
Kurtz, D. W., Schneider, H. & Weiss, W. W., 1985. *Mon. Not. R. astr. Soc.*, **215,** 77.
Ledoux, P., 1951. *Astrophys. J.*, **114,** 373.
Matthews, J., Kurtz, D. W. & Wehlau, W., 1986. *Astrophys. J.*, **300,** 348.
Matthews, J., Kurtz, D. W. & Wehlau, W., 1987. *Astrophys. J.*, **313,** 782.
Matthews, J. M., Wehlau, W. H., Walker, G. A. H. & Yang, S., 1988. *Astrophys. J.*, **324,** 1099.
Mathys, G., 1985. *Astr. Astrophys.*, **151,** 315.
O'Donoghue, D., 1981. *PhD Thesis,* University of Cape Town.
O'Donoghue, D. & Warner, B., 1982. *Mon. Not. R. astr. Soc.*, **200,** 563.
Preston, G. W., 1970. In: *Stellar Rotation,* p. 254, ed. Slettebak, A., Reidel, Dordrecht.
Preston, G. W., 1972. *Astrophys. J.*, **175,** 465.
Schwarzschild, M., 1950. *Astrophys. J.*, **112,** 222.
Shibahashi, H., 1984. *Mem. Soc. astr. Ital.*, **55,** 181.
Shibahashi, H., 1986. In: *Hydrodynamic and Magnetohydrodynamic Problems in the Sun and Stars,* p. 195, ed. Y. Osaki, Department of Astronomy, University of Tokyo.
Shibahashi, H., 1987. *Lecture Notes in Physics,* **274,** 112.
Shibahashi, H. & Saio, H., 1985. *Publs astr. Soc. Japan,* **37,** 245.
Stamford, P. A. & Watson, R. D., 1981. *Astrophys. Space Sci.*, **77,** 131.
Tassoul, M., 1980. *Astrophys. J. Suppl.*, **43,** 469.
Watson, R. D., 1988. *Astrophys. Space Sci.*, **140,** 255.
Weiss, W. W., 1986. *Upper Main Sequence Stars with Anomalous Abundances, IAU colloq. No. 90,* p. 219, eds Cowley, C. R., Dworetsky, M. M. & Megessier, C., Reidel, Dordrecht.
Weiss, W. W. & Schneider, H., 1984. *Astr. Astrophys.*, **135,** 148.
Wolff, S. C. & Morrison, N. D., 1973. *Publs astr. Soc. Pacif.*, **85,** 141.